Accepted Manuscript

Synthesis and evaluation of tetrahydroisoquinoline-benzimidazole hybrids as multifunctional agents for the treatment of Alzheimer's disease

Yuying Fang, Huihao Zhou, Qiong Gu, Jun Xu

PII: S0223-5234(19)30118-7

DOI: https://doi.org/10.1016/j.ejmech.2019.02.008

Reference: EJMECH 11100

To appear in: *European Journal of Medicinal Chemistry*

Received Date: 19 November 2018

Revised Date: 23 January 2019

Accepted Date: 3 February 2019

Please cite this article as: Y. Fang, H. Zhou, Q. Gu, J. Xu, Synthesis and evaluation of tetrahydroisoquinoline-benzimidazole hybrids as multifunctional agents for the treatment of Alzheimer's disease, *European Journal of Medicinal Chemistry* (2019), doi: https://doi.org/10.1016/j.ejmech.2019.02.008.

Graphical abstract

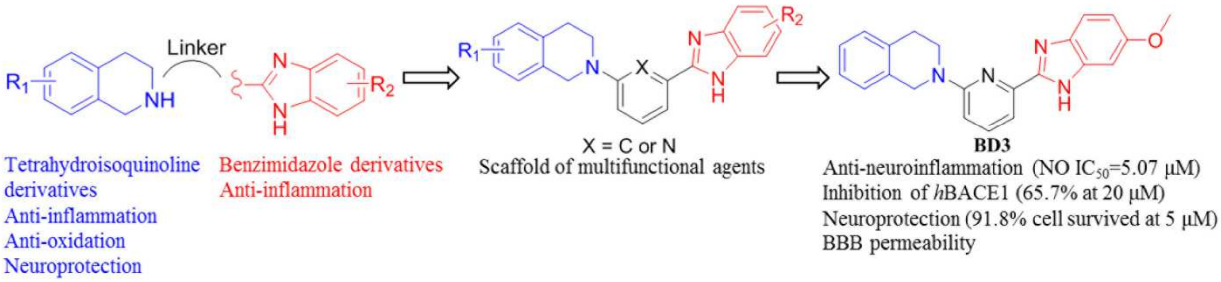

Tetrahydroisoquinoline derivatives
Anti-inflammation
Anti-oxidation
Neuroprotection

Benzimidazole derivatives
Anti-inflammation

Anti-neuroinflammation (NO IC_{50}=5.07 μM)
Inhibition of *h*BACE1 (65.7% at 20 μM)
Neuroprotection (91.8% cell survived at 5 μM)
BBB permeability

Synthesis and evaluation of tetrahydroisoquinoline-benzimidazole hybrids as multifunctional agents for the treatment of Alzheimer's disease

Yuying Fang, Huihao Zhou, Qiong Gu*, Jun Xu*

Research Center for Drug Discovery, School of Pharmaceutical Sciences, Sun Yat-sen University, Guangzhou 510006, People's Republic of China

*Corresponding author

ABSTRACT

A novel series of tetrahydroisoquinoline-benzimidazole hybrids have been designed and synthesized as multifunctional agents against Alzheimer's disease (AD). These compounds were evaluated for their inhibition of neuroinflammation and human *β*-secretase (*h*BACE1), and neuroprotective activity. Among them, compound **BD3** possessed significant anti-neuroinflammatory activity (IC_{50} = 5.07 μM against nitric oxide production) through inhibiting the expression and secretion of proinflammatory cytokines in BV2 cells. Compound **BD3** also exhibited moderate *h*BACE1 inhibitory activity (65.7% inhibition at 20 μM) and potent neuroprotective effect by increasing GSH level and reducing ROS production (91.8% cell viability at 5 μM). Parallel artificial membrane permeation assay demonstrated that **BD3** could cross the blood-brain barrier (BBB). Thus, this study demonstrates that the compounds with tetrahydroisoquinoline-benzimidazole scaffold are potential anti-AD agents, and they are worth for the further development.

Keywords

Tetrahydroisoquinoline-benzimidazole hybrids; Anti-neuroinflammation; BACE1 inhibition; Neuroprotection; Alzheimer's disease

1. Introduction

Alzheimer's disease (AD) [1], a common chronic neurodegenerative disease, is characterized by progressive loss of memory and cognitive functions [2, 3]. With the increasing of population aging and the expanding life span, the number of AD patients is growing. It is estimated that there will be 74.7 million AD patients by 2030 [4]. Currently, only five FDA approved anti-AD drugs are clinically available. They can

only provide temporary and incomplete symptomatic relief [5]. Thus, new anti-AD agents are demanding.

Studies on AD pathogenesis demonstrate that the disease has multiple causes [3, 6-8]. Increasing evidence demonstrates that microglia-dominated neuroinflammation plays a significant role in AD [9]. The chronic and sustained activation of brain microglia cells and the subsequent overproduction of inflammatory mediators, such as nitric oxide (NO), may cause uncontrolled neuroinflammation, elicit neurotoxicity, and contribute to disease pathogenesis. The amyloid cascade hypothesis [10] states that amyloid β (Aβ), in particular Aβ_{42} isoform, has an early and imperative role in AD. BACE1 (β-amyloid precursor protein cleaving enzyme 1), also known as β-secretase, is the key rate-limiting enzyme in the process of Aβ generation. The elevated BACE1 activity has been found in the brains of patients with sporadic AD [11]. BACE1 knockout mice are deficient in Aβ production and have no aberrant phenotype [12]. Therefore, the development of BACE1 inhibitors has been recently pursued [13-15]. In addition, oxidative damage with the overproduction of reactive oxygen species (ROS) may contribute to neuron degeneration and death in this disorder [16].

Since AD has multiple causes, the single targeted drug candidates have high failure rate in clinical trials [17]. Multi-target-directed ligands (MTDLs) [18], aiming to simultaneously target multiple pathological factors (for example neuroinflammation, oxidative damage, and Aβ formation) involved in AD etiology, can be a promising therapeutic strategy.

Benzimidazole exists in several drug candidates, such as antiviral drug Maribavir and antihypertensive drug Telmisartan. Some benzimidazole derivatives are also anti-inflammatory agents [19] and BACE1 inhibitors [20]. In addition, tetrahydroisoquinoline derivatives [21-24] have anti-AD activities, including anti-inflammation, anti-oxidation, and neuroprotection. Therefore, we hypothesize that compounds containing the fragments of tetrahydroisoquinoline and benzimidazole may act as multifunctional drugs against AD. Based on the proposed pharmacophoric model of BACE1 inhibitors [20] and synthetic feasibility, benzene ring and pyridine ring were used as the linker to assemble the two fragments (**Fig. 1**). This resulted in the synthesis of compounds **BD** and **B** series. All the synthesized compounds were evaluated for their activities of anti-neuroinflammation, inhibition of BACE1, neuroprotective effects, and blood-brain barrier (PAMPA-BBB) permeability. This study aims to identify novel multifunctional agents against AD.

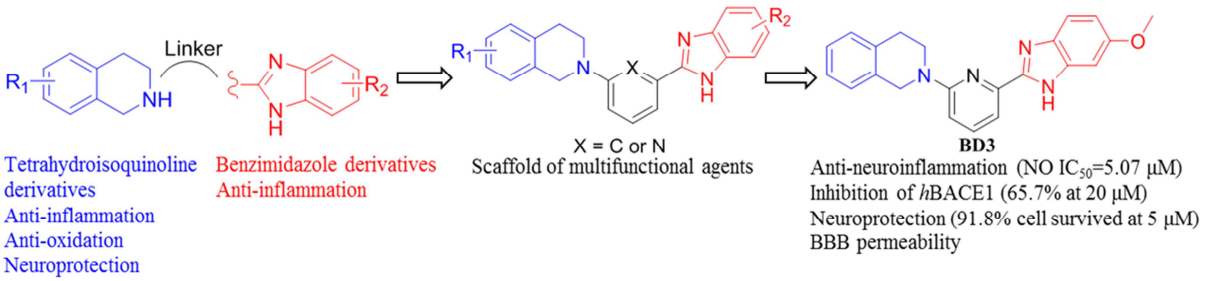

Fig. 1. The scheme of assembling privileged fragments for novel multifunctional compounds against AD.

2. Results and discussion

2.1 Chemistry

The synthetic routes for target compounds of **BD** and **B** series are summarized in **Schemes 1** and **2**. As shown in **Scheme 1**, the key intermediates **12** and **13** were prepared by the reduction of **9** and **10**, which were synthesized via the Aube-Schmidt rearrangement reaction [25] in the presence of NaN_3. The amines **11-13** were mixed with commercially available ethyl 6-bromopicolinate to afford **14-16** through Ullmann coupling reaction in the presence of CuI [26, 27]. Then the intermediates **17-19**, obtained by the hydrolysis of the ester **14-16**, were subjected to couple with the diaminobenzene derivatives followed by acid catalyzed ring closure leading to benzimidazole derivatives **BD1**-**BD11**. For **B** series, the reaction condition is same as that of **BD** series. Twenty-two compounds including **BD** and **B** series were synthesized.

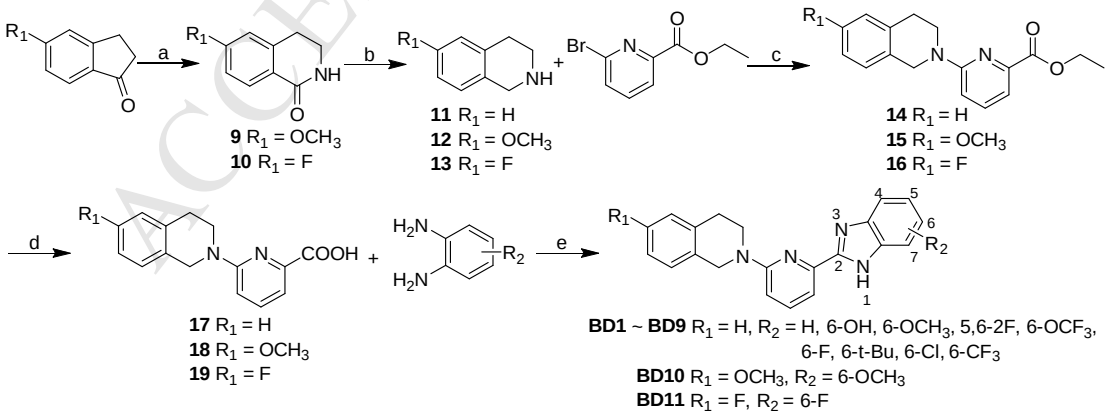

Scheme 1. Synthesis of **BD1**-**BD11**. Reagents and conditions: (a) $MeSO_3H$, NaN_3, DCM, r.t., overnight; (b) $AlLiH_4$, THF, reflux, 4 h; (c) K_2CO_3, CuI, L-proline, DMSO, 80°C, 16 h; (d) LiOH, THF, reflux, 3 h; (e) TBTU, DIPEA, DMF, r.t., 6 h, then AcOH,

reflux, overnight.

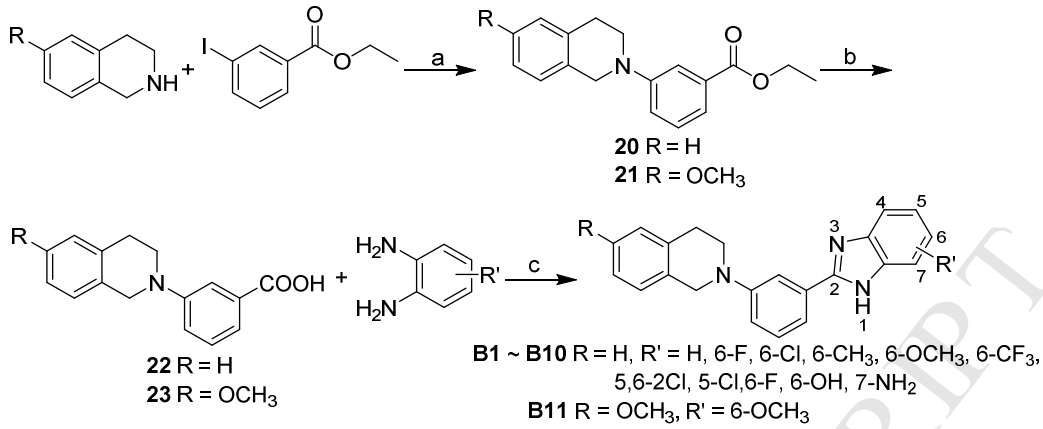

Scheme 2. Synthesis of **B1**-**B11**. Reagents and conditions: (a) K_2CO_3, CuI, L-proline, DMSO, 80°C, 16 h; (b) LiOH, THF, reflux, 3 h; (c) TBTU, DIPEA, DMF, r.t., 6 h, then AcOH, reflux, overnight.

2.2 Effects of anti-neuroinflammation in LPS-induced BV2 microglial cells and SAR study

Anti-neuroinflammatory activities of the synthesized compounds were determined by the Griess assay [28], which detects the NO production in lipopolysaccharide (LPS)-induced BV2 microglia cells. Resveratrol (Res) was used as positive control. Results have been listed in **Table 1**. In comparison to Res, most of the synthesized compounds exhibited potent inhibitory activities against NO production.

For **BD** series, compound **BD1** (R_1 = R_2 = H), with no substituents on tetrahydroisoquinoline and benzimidazole moieties, possesses potent NO inhibitory activity (IC_{50} = 7.33 μM). When substituents at R_2 position on the benzimidazole moiety, compounds **BD2-BD9** (R_1 = H) show similar NO inhibitory activity compared with **BD1**, except for **BD7** (R_2 = *t*-Bu) having the IC_{50} value of more than 10 μM. This demonstrates that the strong electron-donating group tertiary butyl (*t*-Bu) at R_2 position is not beneficial for NO inhibitory activity. Comparing with **BD3** (R_1 = H, R_2 = 6-OCH_3), **BD10** (R_1 = OCH_3, R_2 = 6-OCH_3) exhibit reduced NO inhibitory activity (IC_{50} > 10 μM), which indicates that methoxy group at R_1 position cannot improve inhibitory activity. Compounds **BD6** (R_1 = H, R_2 = 6-F) and **BD11** (R_1 = F, R_2 = 6-F) display nearly the same inhibitory activity with IC_{50} values of 5.70 μM and 6.43 μM. This indicates that the fluorine substituent at the R_1 position has no significant impact

on NO inhibitory activity.

For **B** series, compound **B1** inhibits NO production (IC_{50} = 6.08 μM), which is similar to that of **BD1** (IC_{50} = 7.33 μM). This indicates that the effects of the linker benzene and pyridine on NO inhibitory activity are similar. Compounds **B2-B10** (R = H) have different substituents at R' position on the benzimidazole moiety. The inhibitory activities of most of these compounds do not change much compared with **B1**, while compounds **B3** (R' = 6-Cl), **B8** (R' = 5-Cl, 6-F), and **B10** (R' = 7-NH_2) show reduced NO inhibitory activity with IC_{50} values more than 10 μM. Comparing with **B5** (R = H, R' = 6-OCH_3), compound **B11** (R = OCH_3, R' = 6-OCH_3) displays reduced activity (IC_{50} >10 μM), which demonstrates that methoxy group at the R position is not beneficial for NO inhibition.

Table 1

Inhibitory activities against NO production and BACE1, and BBB permeability ($P_e \times 10^{-6}$ cm s^{-1}) of **BD1**-**BD11** and **B1**-**B11**.

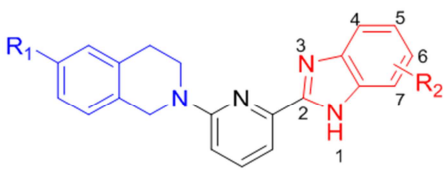

BD1-BD11

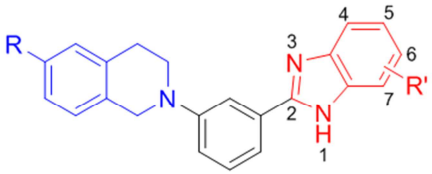

B1-B11

ID	R_1	R_2	NO IC_{50} (μM)[a]	BACE1 inhibition (%)[b]	*Pe* ($\times 10^{-6}$ cm s^{-1})[c]	ID	R	R'	NO IC_{50} (μM)[a]	BACE1 inhibition (%)[b]	*Pe* ($\times 10^{-6}$ cm s^{-1})[c]
BD1	H	H	7.33 ± 0.14	2.1 ± 1.3	15.9 ± 0.8	**B1**	H	H	6.08 ± 0.01	1.5 ± 2.0	8.5 ± 0.7
BD2	H	6-OH	3.80 ± 0.42	2.8 ± 2.8	13.8 ± 0.7	**B2**	H	6-F	5.42 ± 1.21	2.3 ± 1.7	12.6 ± 0.3
BD3	H	6-OCH_3	5.07 ± 0.54	65.7 ± 3.5	16.8 ± 0.3	**B3**	H	6-Cl	> 10	92.7 ± 4.3 (1.3 ± 0.03 μM)[d]	4.9 ± 0.5
BD4	H	5,6-2F	6.58 ± 0.16	0.8 ± 1.2	13.9 ± 0.8	**B4**	H	6-CH_3	5.70 ± 0.94	2.1 ± 1.5	9.6 ± 0.9
BD5	H	6-OCF_3	9.74 ± 0.02	98.7 ± 1.0 (1.1 ± 0.02 μM)[d]	10.0 ± 0.5	**B5**	H	6-OCH_3	8.28 ± 1.13	7.5 ± 3.3	5.6 ± 0.1
BD6	H	6-F	5.70 ± 0.12	5.9 ± 0.4	14.5 ± 0.5	**B6**	H	6-CF_3	7.72 ± 0.89	2.6 ± 1.4	8.7 ± 1.0
BD7	H	6-*t*-Bu	> 10	30.6 ± 2.6	n.d.[e]	**B7**	H	5,6-2Cl	7.93 ± 0.55	1.8 ± 3.2	9.9 ± 0.3
BD8	H	6-Cl	6.94 ± 0.92	95.3 ± 2.3 (1.8 ± 0.3 μM)[d]	16.7 ± 1.2	**B8**	H	5-Cl,6-F	> 10	1.0 ± 2.4	10.1 ± 0.8
BD9	H	6-CF_3	9.33 ± 0.67	90.2 ± 1.9 (3.6 ± 0.05 μM)[d]	5.4 ± 0.5	**B9**	H	6-OH	5.95 ± 0.01	3.0 ± 5.6	8.6 ± 0.9
BD10	OCH_3	6-OCH_3	> 10	25.9 ± 4.2	11.5 ± 0.6	**B10**	H	7-NH_2	> 10	4.8 ± 4.8	13.0 ± 1.1
BD11	F	6-F	6.43 ± 0.62	2.7 ± 2.6	14.0 ± 0.5	**B11**	OCH_3	6-OCH_3	> 10	1.8 ± 1.5	7.6 ± 0.2
Res	-	-	11.1 ± 1.3	-	1.1 ± 0.01	**MK-8931**	-	-	-	98.6 ± 1.9 (20.7 ± 1.2 nM)[d]	16.4 ± 0.3

[a] Concentration (μM) for 50% inhibition of NO release in BV2 cells. [b] The inhibitory activity of BACE1 at the concentration of 20 μM. [c] Compounds were dissolved in DMSO at 5 mg/mL and diluted with PBS/EtOH (70:30). Compounds with permeabilities *Pe* > 4.7 × 10^{-6} cm s^{-1} could cross the BBB by passive diffusion. [d] IC_{50}, the concentration of compounds that inhibited 50% BACE1 enzymatic activity. [e] n.d. Not determined. All values are expressed as the mean ± SD at least three independent experiments.

2.3 Inhibition of human BACE1 activity and SAR study

The BACE1 screening assay utilized in this work was the fluorescence resonance energy transfer (FRET) protocol as previously reported [29]. The inhibitory activities of compounds against BACE1 were tested at the concentration of 20 μM. MK-8931, one of the most potent clinical BACE1 inhibitor, was used as the positive control. As shown in **Table 1**, compounds **B3**, **BD5**, **BD8**, and **BD9** at 20 μM displayed potent inhibitory activities (92.7%, 98.7%, 95.3%, and 90.2%, respectively) comparing to the positive control MK-8931 (98.6%), and the IC_{50} values at 1.3, 1.1, 1.8, and 3.6 μM, respectively. Compound **BD3** showed moderate activity with 65.7% inhibition. Whereas other compounds showed no significant inhibitory activities.

For **BD** series, compounds **BD1**-**BD9**, without substituents at R_1 position (R_1 = H), have different substituents at R_2 position on the benzimidazole moiety. Compounds **BD5** (R_2 = 6-OCF_3), **BD8** (R_2 = 6-Cl), and **BD9** (R_2 = 6-CF_3) exhibit significantly higher inhibitory rate of 98.7%, 95.3%, and 90.2% at 20 μM, respectively. It is worth to mention that **BD5** with 6-OCF_3 at R_2 position is the most potent compound against BACE1. However, compounds **BD2** (R_2 = 6-OH), **BD3** (R_2 = 6-OCH_3), and **BD7** (R_2 = 6-*t*-Bu) exhibit only 2.8%, 65.7%, and 30.6% inhibition at 20 μM, respectively. This indicates that electron-withdrawing groups are beneficial for inhibitory activities comparing with electron-donating groups. Compounds **BD10** and **BD11** do not have improved activities, which suggests that introducing OCH_3 or F group at the R_1 cannot improve inhibitory activities.

For **B** series, compounds **B4** (R' = 6-CH_3), **B5** (R' = 6-OCH_3), **B9** (R' = 6-OH), and **B10** (R' = 7-NH_2), having an electron-donating group at R' on the benzimidazole moiety, display nearly no inhibitory activities (2.1%, 7.5%, 3.0%, and 4.8%, respectively). Compounds **B2** (R' = 6-F) and **B6** (R' = 6-CF_3) with an electron-withdrawing group on the benzimidazole moiety exhibit no inhibitory activities (2.3% and 2.6%), whereas compound **B3** (R' = 6-Cl) exhibits higher activity (92.7%). When two substitutions at the R' position on the benzimidazole moiety, the inhibitory activities of compounds **B7** (R' = 5-Cl, 6-Cl) and **B8** (R' = 5-Cl, 6-F) are not improved (1.8% and 1.0%). When the R group is OCH_3, the activity of compound **B11** nearly remains unchanged (1.8%) compared to **B5** without OCH_3 group at R position (7.5%). This indicates that introducing OCH_3 group at the R does not increase inhibitory activity.

2.4 Neuroprotective activity against glutamate-induced cell death in HT22 cells

Neuronal death is a key characteristic in AD. Glutamate toxicity is a common model to study oxidative stress-induced neuronal cell death [30, 31]. In this model, the HT22 cells (a mouse hippocampal neuron cell line) are exposed to high concentration of extracellular glutamate, which suppresses cystine uptake into the cells via the cystine/glutamate antiporter, leading to the depletion of glutathione (GSH) and accumulation of reactive oxygen species (ROS) and then cell death. To determine whether our compounds could protect neuronal cells from glutamate-induced cytotoxicity, HT22 cells were treated with 5 mM glutamate (Glu) for 24 hours in the presence or absence of different concentrations of compounds (5 μM and 1 μM). The cell viability of neurons was assessed using 3-(4,5-dimethylthiazol-2-yl)-2,5-diphenyl tetrazolium bromide (MTT) analysis.

As shown in **Figs. 2A** and **2B**, only 30% of HT22 cells survived after glutamate treatment for 24 hours, whereas the tested doses of compounds showed different degrees of protection against glutamate-induced cell death. Among **BD** series, compounds **BD1** (R_2 = H), **BD2** (R_2 = 6-OH), **BD3** (R_2 = 6-OCH_3), **BD5** (R_2 = 6-OCF_3), **BD6** (R_2 = 6-F), and **BD11** (R_1 = F, R_2 = 6-F) showed significant protective effect against glutamate-induced cell death at 5 μM with higher cell viability of 80.3%, 98.8%, 91.8%, 62.1%, 67.8%, and 71.1%, respectively. For compounds of **B** series, compounds **B3** (R' = 6-Cl), **B8** (R' = 5-Cl, 6-F), **B10** (R' = 7-NH_2), and **B11** (R = OCH_3, R' = 6-OCH_3) displayed potent protection against glutamate-induced cytotoxicity at 5 μM with higher cell viability of 67.6%, 48.9%, 94.9%, and 93.1%, respectively. It is worth noting that compound **B10**, which contains 7-NH_2 on the benzimidazole moiety, displayed high cell viability of 54.5% at 1 μM.

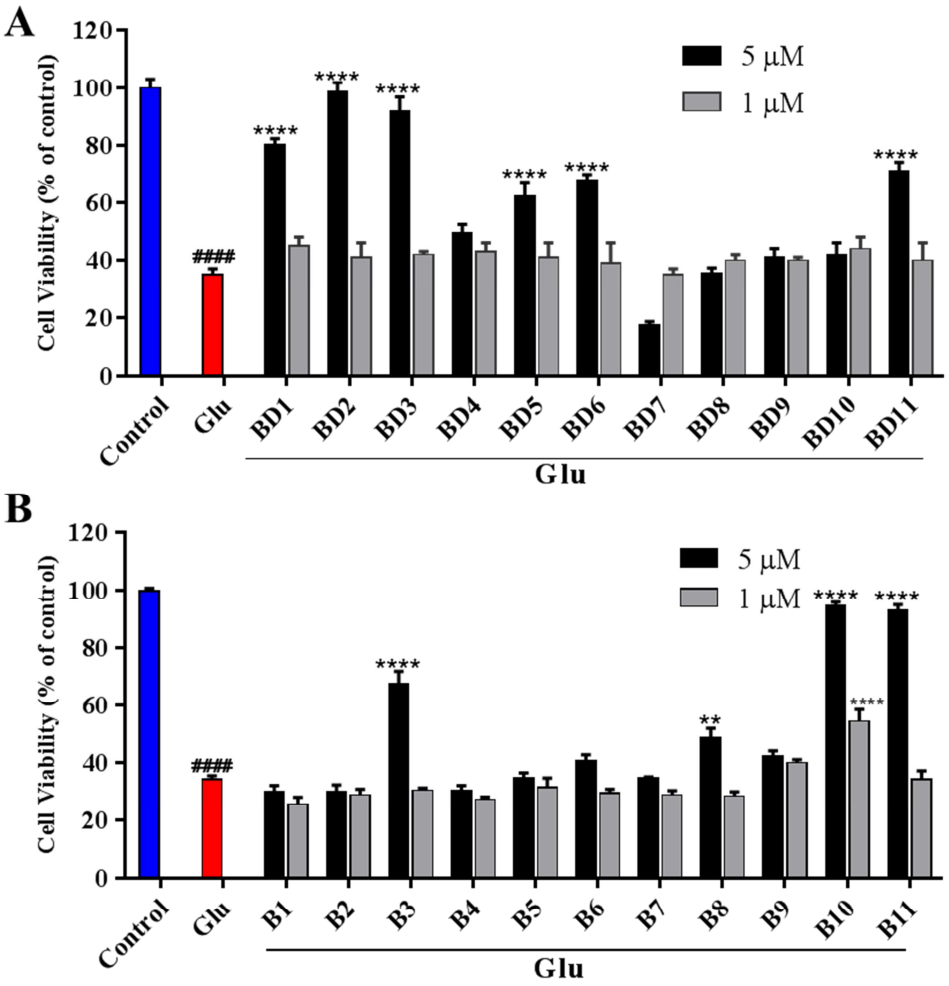

Fig. 2. The protective effects of compounds of **BD** series (A) and **B** series (B) on glutamate-induced cell death. HT22 cells were treated with 5 mM glutamate for 24 hours in the presence or absence of compounds. ####$p < 0.0001$ versus Control group; ****$p < 0.0001$ versus Glu group.

2.5 Blood-brain barrier (BBB) permeability

As the first requirement for successful CNS drugs is to reach their therapeutic targets, screening for the BBB penetration is of great importance. To explore whether our compounds could penetrate into the brain, the compounds were tested with the parallel artificial membrane permeation assay (PAMPA) [32]. This method has the advantage of predicting compounds' passive diffusion through BBB with high throughput and reproducibility. As listed in **Table 1**, all the synthesized compounds showed good BBB permeability.

Based on the overall performance of compound **BD3** (IC_{50} for NO production:

5.07 μM; BACE1 inhibition: 65.7%; potent protection against glutamate-induced toxicity at 5 μM: 91.8%) and its brain BBB penetration, we decided to select compound **BD3** for further investigation.

*2.6 Compound **BD3** inhibits the expression of iNOS and the secretion of proinflammatory cytokines in LPS-induced BV2 cells*

When BV2 cells are stimulated with LPS, the expression of iNOS (inducible nitric oxide synthase) and proinflammatory cytokines such as TNF-α (tumor necrosis factor α) and IL-1β (interleukin 1β) increases. To further evaluate the anti-neuroinflammatory effects of **BD3**, we investigated the protein and mRNA expression of iNOS, TNF-α, and IL-1β through Western blot or ELISA and qPCR. The mRNA levels of iNOS, TNF-α, and IL-1β are generally up-regulated in LPS-stimulated BV2 cells. When treated with various concentrations of **BD3**, the mRNA expressions of iNOS, TNF-α, and IL-1β significantly decreased in a dose-dependent manner in LPS-induced BV2 cells (**Figs. 3E-3G**). Western blot analyses demonstrated that **BD3** significantly decreased the expression of iNOS in LPS-stimulated BV2 cells (**Figs. 3A-3B**). ELISA assays suggested that the levels of TNF-α and IL-1β in the culture medium dramatically increased in LPS-induced BV2 cells. When incubated with different doses of **BD3**, the levels of TNF-α and IL-1β reduced in a concentration-dependent manner (**Figs. 3C-3D**). These results indicate that compound **BD3** exhibits anti-neuroinflammatory activities by inhibiting the protein and mRNA expression of iNOS and proinflammatory cytokines (TNF-α and IL-1β) in LPS-induced BV2 cells.

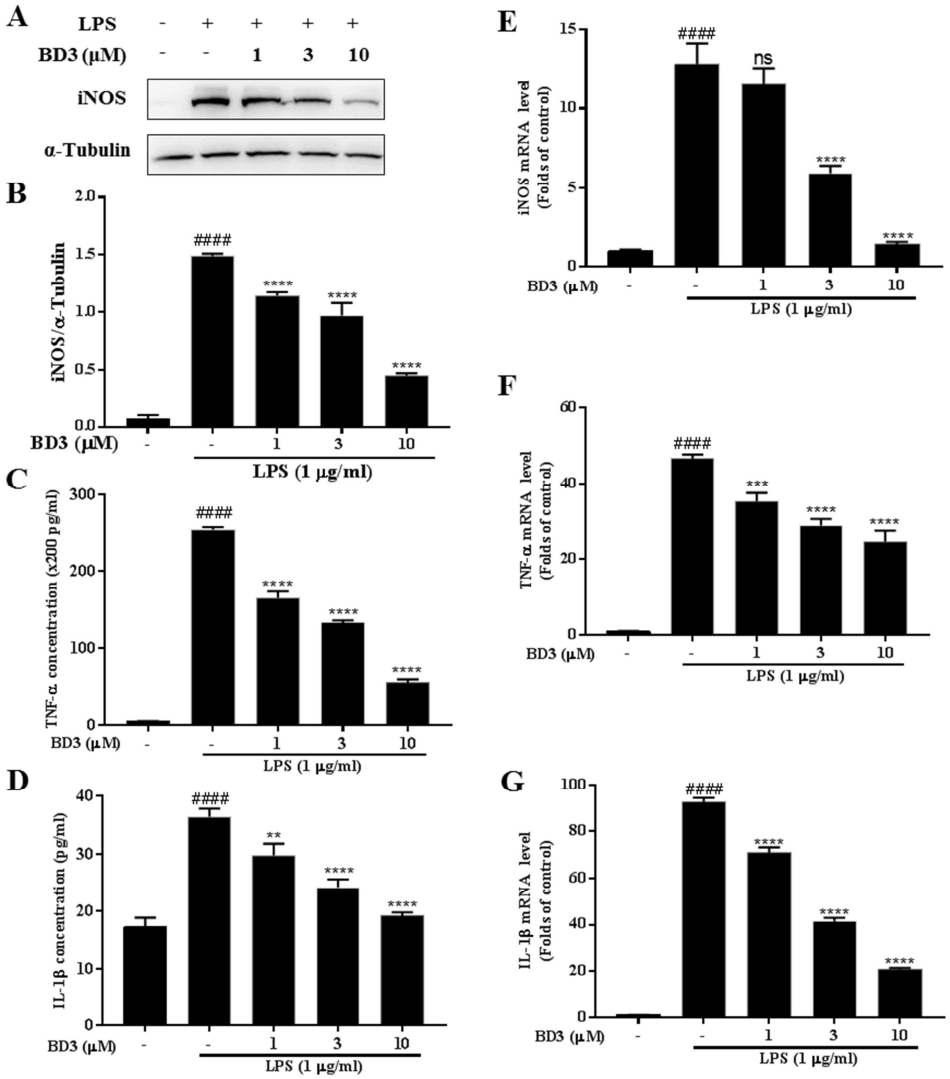

Fig. 3. BD3 suppressed the expression of iNOS and the production of proinflammatory cytokines in LPS-induced BV2 cells. BV2 cells were incubated with different concentrations of **BD3** for 30 minutes, then incubated with LPS (1 μg/mL) for 16 hours. (A) The protein level of iNOS was determined by Western blot. α-Tubulin was used as reference. (B) Quantification of Western blot data. BV2 cells were incubated with **BD3** for 30 minutes, then incubated with LPS (1 μg/mL) for 24 hours. TNF-*α* (C) and IL-1*β* (D) in the supernatants were assayed by ELISA kits. BV2 cells were incubated with **BD3** for 30 minutes, then incubated with LPS (1 μg/mL) for 12 hours. mRNA levels of iNOS (E), TNF-*α* (F) and IL-1*β* (G) were assayed by qPCR. The data are presented as mean ± SEM of three independent experiments. ####p < 0.0001 versus control group, ****p < 0.0001, ***p < 0.001, **p < 0.01, ns (no significance) versus LPS group.

*2.7 Compound **BD3** suppresses glutamate-induced intracellular oxidative stress in HT22 cells*

As shown in **Fig. 2A**, 5 μM **BD3** significantly increased the cell viability of HT22 cells up to 91.8% comparing with glutamate-treated HT22 cells (30%). To further confirm the neuroprotective effects of **BD3** on glutamate-treated HT22 cells, we performed experiments to observe the morphology of HT22 cells treated with or without **BD3**. Exposed to 5 mM glutamate for 24 hours, HT22 cells lost their normal spindle-shaped morphology, and became shrunken and rounded (**Fig. 4A**). While, the cells co-treated with 5 μM **BD3** stayed in normal neurite morphology, similar to the control group. The results were consistent with the data of cell viability (**Fig. 2A**).

To determine whether the protective effect of **BD3** against glutamate-induced toxicity was achieved via inhibiting intracellular oxidative stress, the levels of GSH and ROS in HT22 cells were detected. GSH is an important free radical scavenger in the body. To some extent, the antioxidant ability of the body depends on the level of GSH. The depletion of GSH is a key factor contributing to the glutamate toxicity. After HT22 cells were incubated with 5 mM glutamate for 12 hours in the presence or absence of different concentrations of **BD3**, the contents of GSH were measured using the commercial assay kit. **Fig. 4B** indicates that 5 μM **BD3** can significantly reverse the reduction of GSH level compared to the glutamate-treated cells.

The intracellular ROS was tested using the fluorogenic probe DCFH-DA (2′,7′-dichlorodihydrofluorescein diacetate). After treatment with glutamate in the presence or absence of **BD3**, HT22 cells were incubated with 10 μM DCFH-DA for 30 minutes, then the cells were photographed, and fluorescence intensity was measured. As shown in **Figs. 4C** and **4D**, ROS levels were significantly increased after glutamate treatment for 12 hours, but greatly reduced when HT22 cells were co-treated with 5 μM **BD3**. These data indicate that 5 μM **BD3** can significantly protect cells from glutamate-induced death via antioxidant mechanisms, specifically by increasing the level of GSH and inhibiting the production of ROS.

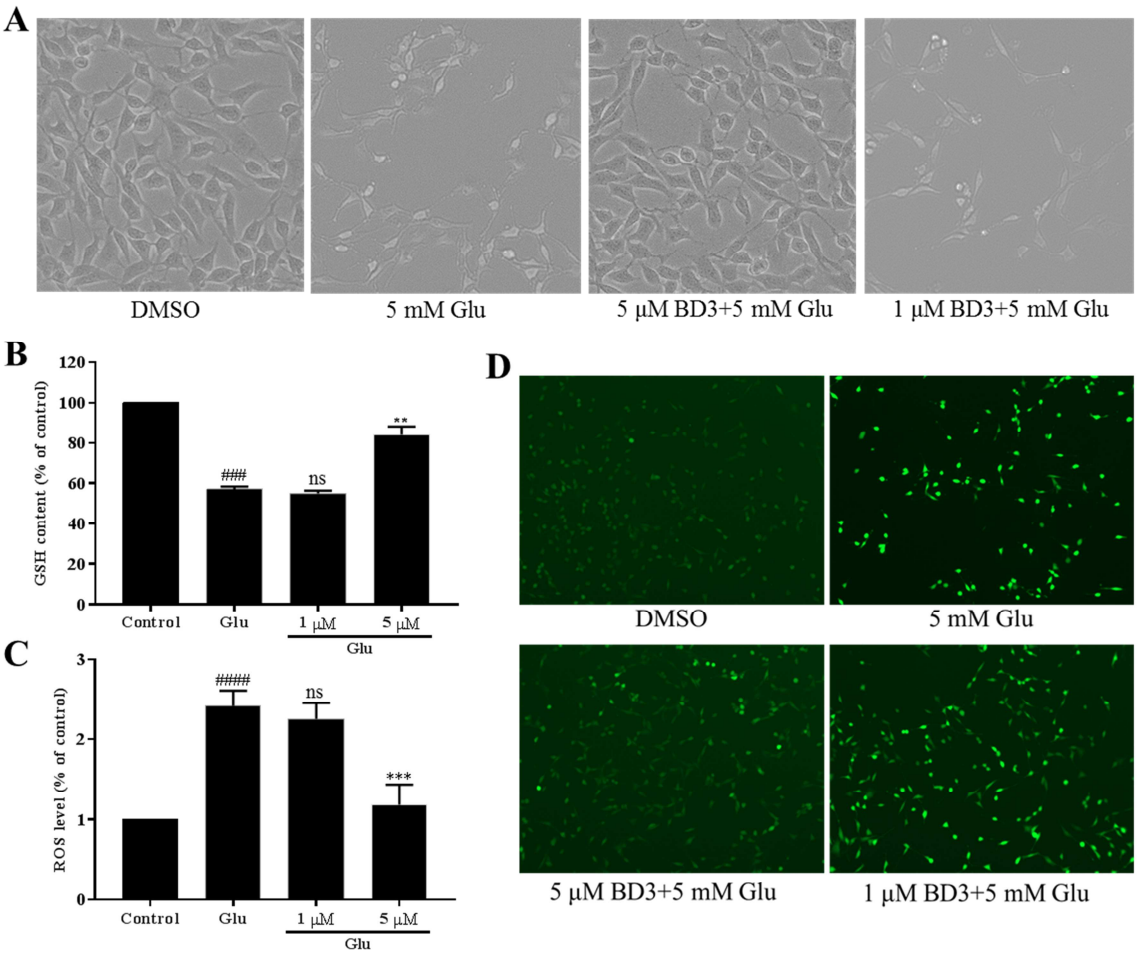

Fig. 4. Compound **BD3** protects HT22 cells from glutamate-induced death via antioxidant mechanisms. HT22 cells were treated with 5 mM glutamate for 24 hours in the presence or absence of **BD3**. (A) The morphology of HT22 cells with different treatments. (B) The levels of GSH were measured using the commercial assay kit. After treated with glutamate in the presence or absence of **BD3** for 12 hours, cells were followed by incubated with 10 μM DCFH-DA for 30 minutes, then (C) the fluorescence intensity was recorded using high content screening system, and (D) cells were photographed. The data are presented as mean ± SEM of three independent experiments. ####$p < 0.0001$, ###$p < 0.001$ versus Control group; ***$p < 0.001$, **$p < 0.01$, ns (no significance) versus Glu group.

*2.8 Binding mode of **BD3** with BACE1 in silico*

Compound **BD3** was docked into the binding pocket of *h*BACE1 (PDB ID:

2B8L) with Glide extra precision (XP). As shown in **Fig. 5**, the NH of the benzimidazole moiety of the compound formed a hydrogen bond with Asp32 in the catalytic pocket and the oxygen atom of the OCH_3 group formed a hydrogen bond with a water molecule. The pyridine ring of **BD3** interacted with Phe108 via π-π stacking and the protonation of nitrogen atom of the pyridine ring produced a hydrogen bond between Gly230 and the hydrogen atom.

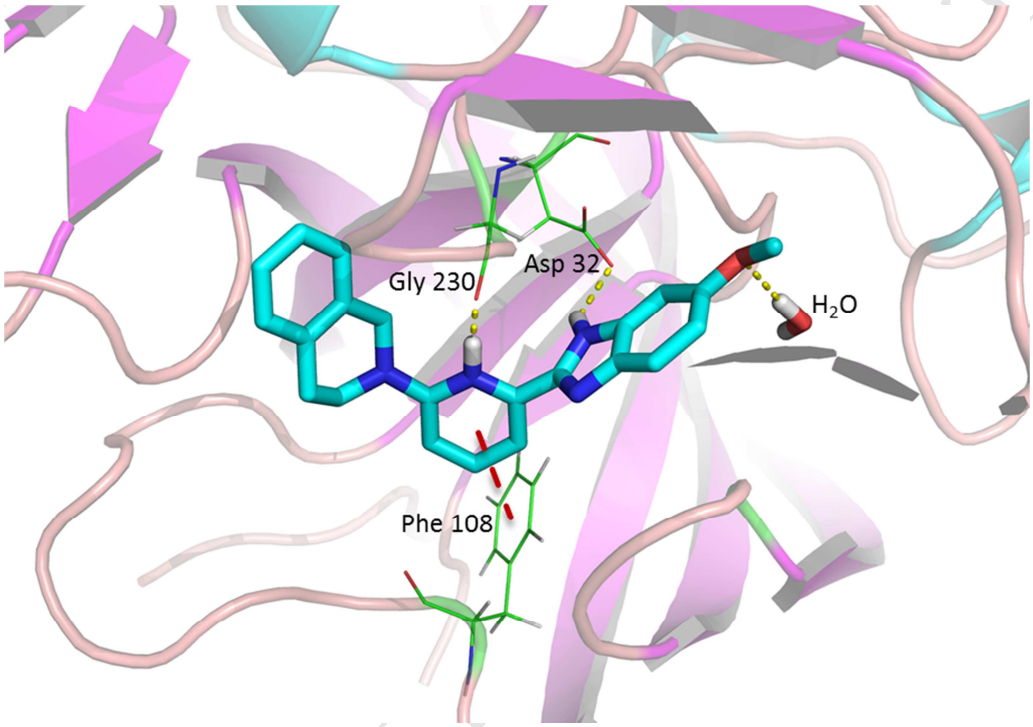

Fig. 5. The proposed binding model of **BD3**-BACE1 complex. The yellow dash lines represent hydrogen bonds and the red dash lines represent π-π stacking interaction.

*2.9 ADMET properties for compound **BD3***

To investigate the drug-like profiles of **BD3**, the ADMET properties were estimated using Discovery Studio 3.5 software package (**Table 2**). The results indicate that **BD3** can have high blood-brain penetration, good absorption, no liver toxicity, and no inhibition of CYP2D6. **BD3** could easily bind to carrier proteins in the blood, however, the solubility of **BD3** is low. Hence, the structure of **BD3** need to be further optimized regarding to its pharmacokinetic profile.

Table 2

ADMET properties for **BD3**

Structure	BBB[a]	Absorption[b]	Solubility[c]	Hepatotoxicity[d]	CYP2D6[e]	PPB[f]

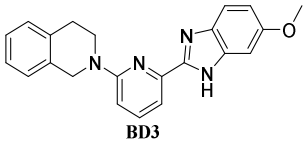 BD3	High	Good	Very low, but possible	Nontoxic	Non-inhibitor	True

[a] BBB predicts blood-brain penetration after oral administration.; [b] Absorption predicts human intestinal absorption (HIA) after oral administration.; [c] Solubility predicts the solubility of each compound in water at 25°C.; [d] Hepatotoxicity predicts potential liver toxicity of compounds.; [e] CYP2D6 (cytochrome P450 2D6) predicts CYP2D6 enzyme inhibition using 2D chemical structure.; [f] PPB (plasma protein binding) predicts whether a compound is likely to be highly bound (>= 90% bound) to carrier proteins in the blood.

3 Conclusion

This work demonstrates that multifunctional agents against AD can be discovered by assembling the fragments benzimidazole and tetrahydroisoquinoline. This is another example that develops lead compounds through assembling two active fragments [33]. Among the synthesized compounds, some compounds exhibit great inhibition of neuroinflammation and *h*BACE1, as well as good neuroprotective effect and BBB penetration. *In vitro* and *in silico* experiments indicate that **BD3** can inhibit BACE1 by interacting with the catalytic pocket in BACE1. **BD3** showed anti-neuroinflammatory activity through suppressing the expressions of inflammatory proteins and genes. **BD3** also possessed significant protective effects on neuronal cells against the glutamate-induced cytotoxicity in HT22 cells by preventing the ROS production and increasing the GSH level. Moreover, **BD3** could penetrate BBB. Therefore, **BD3** could be a lead for further optimization as a multifunctional agent against Alzheimer's disease.

4 Experimental section

4.1 Chemistry

4.1.1 Materials and equipment. Reagents were used without further purification unless specified. ^{1}H and ^{13}C NMR spectra were recorded using tetramethylsilane (TMS) as the internal standard on a Bruker Ascend™ 400 or Bruker Ascend™ 500 spectrometer. Coupling constants are given in Hz. High-resolution mass spectra were obtained using a Shimadzu LCMS-IT-TOF mass spectrometer. Mass spectra (MS) were recorded on a Shimadzu LCMS-2010A instrument with an ESI source. Flash

column chromatography was performed using silica gel (200–300 mesh) purchased from Qingdao Haiyang Chemical Co. Ltd. All reaction progress was monitored by thin layer chromatography (TLC) on precoated silica gel GF254 (Qingdao Haiyang Chemical Co. Ltd) and the spots were detected under UV light (254 nm).

*4.1.2 General procedure for the synthesis of intermediates **9** and **10***

According to previously reported method [26], 5-methoxy-1-indanone (4.30 g, 26.6 mmol) or 5-fluoro-1-indanone (4.00 g, 26.6 mmol) were dissolved in the mixed solvent of CH_2Cl_2 (40 mL) and $MeSO_3H$ (methanesulfonic acid, 40 mL). NaN_3 (3.46 g, 53.2 mmol) was added slowly in an ice-water bath. Then the mixture was stirred overnight at room temperature. In an ice-water bath, 20% NaOH (aq) was added to make the solution neutral. The aqueous solution was extracted with CH_2Cl_2 and the obtained organic layer was combined, washed with brine, dried over $MgSO_4$ and concentrated. The residue was purified by silica gel flash chromatography (EtOAc/hexane = 2/1).

*6-methoxy-3,4-dihydroisoquinolin-1(2H)-one (**9**)*. White solid (2.82 g, 60%). ^{1}H NMR (400 MHz, CD_3OD) δ 7.93 (d, J = 8.6 Hz, 1H), 6.95 (dd, J = 8.6, 2.4 Hz, 1H), 6.89 (d, J = 1.8 Hz, 1H), 3.91 (s, 3H), 3.54 (t, J = 6.7 Hz, 2H), 3.02 (t, J = 6.7 Hz, 2H); ESI-MS: *m/z* 176.0 $[M-H]^-$.

*6-fluoro-3,4-dihydroisoquinolin-1(2H)-one (**10**)*. White solid (2.32 g, 53%). ^{1}H NMR (400 MHz, CD_3OD) δ 8.03 (dd, J = 8.3, 5.9 Hz, 1H), 7.20 - 7.06 (m, 2H), 3.56 (t, J = 6.7 Hz, 2H), 3.05 (t, J = 6.7 Hz, 2H); ESI-MS: *m/z* 164.0 $[M-H]^-$.

*4.1.3 General procedure for the synthesis of intermediates **12** and **13***

According to previously reported method [34], compound **9** (1.77 g, 10 mmol) or **10** (1.65 g, 10 mmol) was dissolved in dry THF (50 mL). Then in an ice-water bath, it was added dropwise to a solution of $LiAlH_4$ in dry THF (1 mol/L, 20 mL) under N_2 environment. The mixture was stirred at reflux for 4 h, and then quenched by the sequential addition of THF and 30% NaOH solution in the ice-water bath. The reaction mixture was filtered through celite and washed with MeOH. The residue was evaporated *in vacuum* and purified by silica gel flash chromatography (EtOAc/MeOH = 10/1).

*6-methoxy-1,2,3,4-tetrahydroisoquinoline (**12**)*. White oil (0.81 g, 50%). ^{1}H NMR (400 MHz, CD_3OD) δ 7.01 (d, J = 8.4 Hz, 1H), 6.76 (d, J = 8.4 Hz, 1H), 6.72 (s, 1H), 3.99 (s, 2H), 3.79 (s, 3H), 3.17 (t, J = 6.0 Hz, 2H), 2.89 (t, J = 5.8 Hz, 2H); ESI-MS: *m/z* 162.1 $[M-H]^-$.

*6-fluoro-1,2,3,4-tetrahydroisoquinoline (**13**)*. White oil (0.95 g, 63%). ^{1}H NMR (400 MHz, CD_3OD) δ 7.14 - 7.08 (m, 1H), 6.95 - 6.85 (m, 2H), 4.04 (s, 2H), 3.18 (t, J = 6.1 Hz, 2H), 2.92 (t, J = 5.9 Hz, 2H); ESI-MS: *m/z* 150.0 $[M-H]^-$.

*4.1.4 General procedure for the synthesis of intermediates **14-16**, **20**, and **21***

To a dried sealed vessel was added 1,2,3,4-tetrahydroisoquinoline (5 mL, 40 mmol), anhydrous K_2CO_3 (8.34 g, 60 mmol), CuI (0.8 g, 4 mmol), L-Proline (0.92 g, 8 mmol), ethyl 6-bromopicolinate (4.32 g, 20 mmol), and DMSO (25 mL). Then the mixture was stirred at 80°C for 16 h under N_2 environment. After cooling to room temperature, water (100 mL) was added and extracted with EtOAc. Then, the combined organic layer was dried over $MgSO_4$, filtered, and concentrated. The residue was purified by silica gel flash chromatography (hexane/EtOAc = 5/1) to provide compound **14** as a white oil (3.94 g, 70%).

*Ethyl 6-(3,4-dihydroisoquinolin-2(1H)-yl)picolinate (**14**)*. ^{1}H NMR (400 MHz, $CDCl_3$) δ 7.59 (t, J = 7.9 Hz, 1H), 7.40 (d, J = 7.3 Hz, 1H), 7.24 - 7.16 (m, 4H), 6.83 (d, J = 8.6 Hz, 1H), 4.76 (s, 2H), 4.42 (q, J = 7.2 Hz, 2H), 3.94 (t, J = 5.8 Hz, 2H), 2.98 (t, J = 5.8 Hz, 2H), 1.43 (t, J = 7.1 Hz, 3H) ; ESI-MS: *m/z* 281.1 $[M-H]^-$.

*Ethyl 6-(6-methoxy-3,4-dihydroisoquinolin-2(1H)-yl)picolinate (**15**)*. White oil, 70%. ^{1}H NMR (400 MHz, $CDCl_3$) δ 7.58 (t, J = 7.9 Hz, 1H), 7.39 (d, J = 7.3 Hz, 1H), 7.13 (d, J = 8.4 Hz, 1H), 6.81 (d, J = 8.6 Hz, 1H), 6.78 (dd, J = 8.4, 2.4 Hz, 1H), 6.72 (s, 1H), 4.68 (s, 2H), 4.42 (q, J = 7.1 Hz, 2H), 3.92 (t, J = 5.8 Hz, 2H), 3.80 (s, 3H), 2.95 (t, J = 5.8 Hz, 2H), 1.42 (t, J = 7.1 Hz, 3H); ESI-MS: *m/z* 311.1 $[M-H]^-$.

*Ethyl 6-(6-fluoro-3,4-dihydroisoquinolin-2(1H)-yl)picolinate (**16**)*. Yellow oil, 72%. ^{1}H NMR (400 MHz, $CDCl_3$) δ 7.60 (dd, J = 8.4, 7.4 Hz, 1H), 7.41 (d, J = 7.3 Hz, 1H), 7.17 (dd, J = 8.1, 5.7 Hz, 1H), 6.93 - 6.85(m, 2H), 6.82 (d, J = 8.5 Hz, 1H), 4.72 (s, 2H), 4.42 (q, J = 7.1 Hz, 2H), 3.91 (t, J = 5.9 Hz, 2H), 2.96 (t, J = 5.8 Hz, 2H), 1.42 (t, J = 7.1 Hz, 3H); ESI-MS: *m/z* 299.1 $[M-H]^-$.

*Ethyl 3-(3,4-dihydroisoquinolin-2(1H)-yl)benzoate (**20**)*. White oil, 75%. ^{1}H NMR (400 MHz, $CDCl_3$) δ 7.66 (dd, J = 2.5, 1.6 Hz, 1H), 7.50 (d, J = 7.6 Hz, 1H), 7.34 (t, J = 7.9 Hz, 1H), 7.22 - 7.12(m, 5H), 4.46 (s, 2H), 4.39 (q, J = 7.1 Hz, 2H), 3.61 (t, J = 5.9 Hz, 2H), 3.01 (t, J = 5.8 Hz, 2H), 1.41 (t, J = 7.1 Hz, 3H); ESI-MS: *m/z* 280.1 $[M-H]^-$.

*Ethyl 3-(6-methoxy-3,4-dihydroisoquinolin-2(1H)-yl)benzoate (**21**)*. White oil, 70%. ^{1}H NMR (400 MHz, $CDCl_3$) δ 7.68 (s, 1H), 7.54 (d, J = 7.3 Hz, 1H), 7.35 (t, J = 7.9 Hz, 1H), 7.25 - 7.18 (m, 1H), 7.09 (d, J = 8.4 Hz, 1H), 6.78 (dd, J = 8.4, 2.6 Hz, 1H),

6.71 (d, *J* = 2.5 Hz, 1H), 4.42 (s, 2H), 4.38 (q, *J* = 7.1 Hz, 2H), 3.80 (s, 3H), 3.61 (t, *J* = 5.9 Hz, 2H), 3.00 (t, *J* = 5.5 Hz, 2H), 1.40 (t, *J* = 7.1 Hz, 3H); ESI-MS: *m/z* 310.1 $[M-H]^-$.

*4.1.5 General procedure for the synthesis of intermediates **17-19**, **22**, and **23***

The intermediate **14** (2.82 g, 10 mmol) was dissolved in THF (50 mL). Then LiOH (1.19 g, 50 mmol) and the mixture of EtOH/H_2O = 5:1 (5 mL) were added into the round flask. After stirred at reflux for 3 h, the solvent was evaporated *in vacuo*. A small amount of ice-water was added to dissolve the residue. The 1N HCl aqueous solution was added slowly to make the solution neutral. The resulting precipitate was isolated by filtration and dried under vacuum to afford compound **17**.

*6-(3,4-dihydroisoquinolin-2(1H)-yl)picolinic acid (**17**).* Light yellow solid, 92%. ^{1}H NMR (400 MHz, CD_3OD) δ 8.12 (dd, *J* = 9.1, 7.3 Hz, 1H), 7.68 (d, *J* = 9.2 Hz, 1H), 7.63 (d, *J* = 7.1 Hz, 1H), 7.37 - 7.28 (m, 4H), 4.92 (s, 2H), 3.97 (t, *J* = 5.9 Hz, 2H), 3.15 (t, *J* = 5.9 Hz, 2H); ESI-MS: *m/z* 253.1 $[M-H]^-$.

*6-(6-methoxy-3,4-dihydroisoquinolin-2(1H)-yl)picolinic acid (**18**)*. Light yellow solid, 70%. ^{1}H NMR (400 MHz, $CDCl_3$) δ 7.70 (t, *J* = 7.8 Hz, 1H), 7.51 (d, *J* = 7.1 Hz, 1H), 7.13 (d, *J* = 8.3 Hz, 1H), 6.93 (d, *J* = 8.6 Hz, 1H), 6.80 (d, *J* = 8.3 Hz, 1H), 6.75 (s, 1H), 4.65 (s, 2H), 3.86 - 3.76 (m, 5H), 2.97 (t, *J* = 5.5 Hz, 2H); ESI-MS: *m/z* 283.1 $[M-H]^-$.

*6-(6-fluoro-3,4-dihydroisoquinolin-2(1H)-yl)picolinic acid (**19**)*. Yellow solid, 80%. ^{1}H NMR (400 MHz, $CDCl_3$) δ 7.60 (dd, *J* = 8.4, 7.4 Hz, 1H), 7.41 (d, *J* = 7.3 Hz, 1H), 7.17 (dd, *J* = 8.1, 5.7 Hz, 1H), 6.93 - 6.85(m, 2H), 6.82 (d, *J* = 8.5 Hz, 1H), 4.72 (s, 2H), 3.91 (t, *J* = 5.9 Hz, 2H), 2.96 (t, *J* = 5.8 Hz, 2H); ESI-MS: *m/z* 271.1 $[M-H]^-$.

*3-(3,4-dihydroisoquinolin-2(1H)-yl)benzoic acid (**22**).* Light yellow solid, 65%. ^{1}H NMR (400 MHz, $CDCl_3$) δ 7.71 (s, 1H), 7.58 (d, *J* = 7.6 Hz, 1H), 7.38 (t, *J* = 7.9 Hz, 1H), 7.24 - 7.17 (m, 5H), 4.48 (s, 2H), 3.64 (t, *J* = 5.9 Hz, 2H), 3.02 (t, *J* = 5.8 Hz, 2H) ; ESI-MS: *m/z* 252.1 $[M-H]^-$.

*3-(6-methoxy-3,4-dihydroisoquinolin-2(1H)-yl)benzoic acid (**23**)*. Light yellow solid, 80%. ^{1}H NMR (400 MHz, $CDCl_3$) δ 7.67 (s, 1H), 7.54 (d, *J* = 7.6 Hz, 1H), 7.36 (t, *J* = 7.9 Hz, 1H), 7.18 (dd, *J* = 8.1, 2.3 Hz, 1H), 7.10 (d, *J* = 8.4 Hz, 1H), 6.78 (dd, *J* = 8.4, 2.6 Hz, 1H), 6.72 (d, *J* = 2.4 Hz, 1H), 4.41 (s, 2H), 3.80 (s, 3H), 3.60 (t, *J* = 5.9 Hz, 2H), 2.98 (t, *J* = 5.7 Hz, 2H); ESI-MS: *m/z* 282.1 $[M-H]^-$.

*4.1.6 General procedure for the synthesis of **BD1**-**BD11** and **B1**-**B11***

To a solution of the desired carboxylic acids (**17**, **18**, **19**, **22** or **23**) (1 mmol) in

DMF (5 mL) at 0°C was added DIPEA (0.21 mL, 1.2 mmol). TBTU（385 mg, 1.2 mmol）was added and the resulting mixture were stirred at 0°C for 30 minutes. Then the desired diaminobenzene derivative (1.1 mmol) was added. The mixture was stirred at room temperature for 6 h and then quenched with ice-water. The precipitated solid was filtered, washed with water, and dissolved in EtOAc. The organic layer was washed with a 1 N HCl aqueous solution, then with a saturated $NaHCO_3$ aqueous solution and finally H_2O, dried over $MgSO_4$, and concentrated *in vacuo*, which was used in the next step without further purification. To the appropriate amide was added AcOH (10 mL), and the mixture was refluxed overnight, cooled to room temperature and concentrated under reduced pressure. The residue was purified by flash chromatography.

*4.1.6.1 2-(6-(1H-benzo[d]imidazol-2-yl)pyridin-2-yl)-1,2,3,4-tetrahydroisoquinoline (**BD1**).*

Following the general procedure above, **BD1** was obtained as a white solid (60%). ^{1}H NMR (400 MHz, $CDCl_3$) δ 10.45 (s, 1H), 7.84 (s, 1H), 7.77 (d, J = 7.3 Hz, 1H), 7.66 (t, J = 7.8 Hz, 1H), 7.55 (s, 1H), 7.32 - 7.27 (m, 2H), 7.25 - 7.17 (m, 4H), 6.77 (d, J = 8.4 Hz, 1H), 4.79 (s, 2H), 3.95 (t, J = 5.9 Hz, 2H), 3.01 (t, J = 5.8 Hz, 2H). ^{13}C NMR (100 MHz, DMSO-d_6) δ 157.7, 150.7, 145.5, 138.1, 138.0, 134.8, 134.1, 128.0, 127.8, 127.0, 126.0, 125.8, 125.5, 122.1, 115.0, 114.9, 109.8, 107.5, 46.3, 41.8, 27.8. HR-ESI-MS: $[M+H]^+$ m/z = 327.1604, calcd for $C_{21}H_{18}N_4$, found 327.1585.

*4.1.6.2 2-(6-(3,4-dihydroisoquinolin-2(1H)-yl)pyridin-2-yl)-1H-benzo[d]imidazol-6-ol (**BD2**).*

Following the general procedure above, **BD3** was obtained firstly. Then compound **BD3** was dissolved in HBr (48% in H_2O). The mixture was stirred at 120 °C for 3 h and then concentrated *in vacuo*. Compound **BD2** was obtained as a yellow solid (50%). ^{1}H NMR (400 MHz, CD_3OD) δ 7.84 (dd, J = 8.7, 7.3 Hz, 1H), 7.67 (d, J = 9.1 Hz, 1H), 7.48 (d, J = 7.3 Hz, 1H), 7.31 (d, J = 7.0 Hz, 1H), 7.25 - 7.12 (m, 6H), 4.90 (s, 2H), 4.03 (t, J = 5.9 Hz, 2H), 3.03 (t, J = 5.9 Hz, 2H). ^{13}C NMR (100 MHz, CD_3OD) δ 159.9, 158.8, 148.9, 140.6, 139.9, 136.5, 135.2, 134.2, 129.3, 127.7, 127.5, 127.3, 126.4, 118.2, 115.8, 112.3, 112.0, 99.3, 47.8, 43.7, 29.8. HR-ESI-MS: $[M+H]^+$ m/z = 343.1553, calcd for $C_{21}H_{18}N_4O$, found 343.1522.

4.1.6.3

*2-(6-(6-methoxy-1H-benzo[d]imidazol-2-yl)pyridin-2-yl)-1,2,3,4-tetrahydroisoquinoline (**BD3**).*

Following the general procedure above, **BD3** was obtained as a white solid (22%). ^{1}H NMR (400 MHz, DMSO-d_6) δ 7.64 (t, J = 7.9 Hz, 1H), 7.48 (d, J = 7.3 Hz, 2H), 7.25 (d, J = 7.4 Hz, 1H), 7.18 - 7.05 (m, 4H), 6.86 (d, J = 8.5 Hz, 1H), 6.81 (d, J = 7.9 Hz, 1H), 4.79 (s, 2H), 3.93 (t, J = 5.5 Hz, 2H), 3.76 (s, 3H), 2.90 (t, J = 5.4 Hz, 2H). ^{13}C NMR (100 MHz, DMSO-d_6) δ 157.8, 156.2, 150.5, 146.4, 138.5, 135.1, 134.5, 128.4, 126.5, 126.2, 125.9, 119.7, 111.5, 109.3, 107.2, 94.7, 55.3, 46.5, 41.9, 28.1. HR-ESI-MS: $[M+H]^+$ m/z = 357.1710, calcd for $C_{22}H_{20}N_4O$, found 357.1688.

4.1.6.4

*2-(6-(5,6-difluoro-1H-benzo[d]imidazol-2-yl)pyridin-2-yl)-1,2,3,4-tetrahydroisoquinoline (**BD4**).*

Following the general procedure above, **BD4** was obtained as a white solid (25%). ^{1}H NMR (400 MHz, $CDCl_3$) δ 10.37 (s, 1H), 7.81 - 7.50 (m, 4H), 7.41 - 7.28 (m, 2H), 7.24 (s, 3H), 6.86 - 6.73 (m, 1H), 4.80 (d, J = 11.6 Hz, 2H), 3.95 (t, J = 5.9 Hz, 2H), 3.03 (t, J = 5.8 Hz, 2H). ^{13}C NMR (100 MHz, DMSO-d_6) δ 157.9, 152.9, 148.4, 148.2, 146.0, 145.9, 145.0, 138.6, 135.0, 134.3, 128.4, 126.4, 126.2, 126.0, 110.0, 108.3, 103.1, 102.8, 46.5, 41.8, 28.1. HR-ESI-MS: $[M+H]^+$ m/z = 363.1416, calcd for $C_{21}H_{16}F_2N_4$, found 363.1395.

4.1.6.5

*2-(6-(6-(trifluoromethoxy)-1H-benzo[d]imidazol-2-yl)pyridin-2-yl)-1,2,3,4-tetrahydroisoquinoline (**BD5**).*

Following the general procedure above, **BD5** was obtained as a white solid (20%). ^{1}H NMR (400 MHz, $CDCl_3$) δ 7.73 (d, J = 8.8 Hz, 1H), 7.69 - 7.57 (m, 2H), 7.46 (d, J = 8.7 Hz, 1H), 7.38 (s, 1H), 7.19 - 7.07 (m, 4H), 6.74 (d, J = 8.4 Hz, 1H), 4.73 (s, 2H), 3.89 (t, J = 5.8 Hz, 2H), 2.96 (t, J = 5.8 Hz, 2H). ^{13}C NMR (100 MHz, DMSO-d_6) δ 157.9, 153.3, 145.5, 143.9, 139.7, 138.6, 135.0, 134.3, 128.3, 127.5, 126.5, 126.2, 125.9, 120.6, 120.4 (q, J = 255.2 Hz), 117.8, 116.2, 110.1, 108.2, 46.5, 41.9, 28.1. HR-ESI-MS: $[M+H]^+$ m/z = 411.1427, calcd for $C_{22}H_{17}F_3N_4O$, found 411.1421.

4.1.6.6

*2-(6-(6-fluoro-1H-benzo[d]imidazol-2-yl)pyridin-2-yl)-1,2,3,4-tetrahydroisoquinoline (**BD6**).*

Following the general procedure above, **BD6** was obtained as a white solid (20%). ^{1}H NMR (400 MHz, $CDCl_3$) δ 10.34 (s, 1H), 7.78 - 7.61 (m, 3H), 7.52 - 7.43 (m, 1H), 7.25 – 7.19 (m, 4H), 7.09 - 7.00 (m, 1H), 6.78 (dd, J = 8.3, 3.6 Hz, 1H), 4.79 (s, 2H), 3.96 (t, J = 5.9 Hz, 2H), 3.02 (t, J = 5.9 Hz, 2H). ^{13}C NMR (100 MHz, DMSO-d_6) δ 160.0, 157.9, 157.7, 152.3, 145.3, 138.6 (2C), 135.0, 134.3, 128.3, 126.5, 126.2, 125.9, 111.0, 110.7, 110.0 (2C), 108.1, 46.5, 41.8, 28.1. HR-ESI-MS: $[M+H]^+$ *m/z* = 345.1510, calcd for $C_{21}H_{17}FN_4$, found 345.1488.

4.1.6.7

*2-(6-(6-(tert-butyl)-1H-benzo[d]imidazol-2-yl)pyridin-2-yl)-1,2,3,4-tetrahydroisoquinoline (**BD7**).*

Following the general procedure above, **BD7** was obtained as a white solid (50%). ^{1}H NMR (400 MHz, DMSO-d_6) δ 12.50 (s, 1H), 7.74 - 7.68 (m, 1H), 7.63 - 7.52 (m, 3H), 7.32 (d, J = 7.4 Hz, 2H), 7.26 - 7.17 (m, 3H), 6.96 (d, J = 8.5 Hz, 2H), 4.86 (s, 2H), 4.01 (t, J = 5.9 Hz, 2H), 2.97 (t, J = 5.8 Hz, 2H), 1.37 (s, 9H). ^{13}C NMR (100 MHz, DMSO-d_6) δ 157.66, 151.03, 146.32, 144.90, 137.94, 134.82, 134.17, 127.90, 126.06, 125.82, 125.50, 119.74, 119.69, 119.53, 109.39, 106.99, 46.36, 41.84, 34.11, 31.28 (3C), 27.87. HR-ESI-MS: $[M+H]^+$ *m/z* = 383.2230, calcd for $C_{25}H_{26}N_4$, found 383.2210.

4.1.6.8

*2-(6-(6-chloro-1H-benzo[d]imidazol-2-yl)pyridin-2-yl)-1,2,3,4-tetrahydroisoquinoline (**BD8**).*

Following the general procedure above, **BD8** was obtained as a white solid (40%). ^{1}H NMR (400 MHz, $CDCl_3$) δ 7.73 (d, J = 7.3 Hz, 1H), 7.67 (t, J = 7.8 Hz, 2H), 7.63 - 7.55(m, 1H), 7.27 (d, J = 2.5 Hz, 1H), 7.25 - 7.20 (m, 4H), 6.79 (d, J = 8.4 Hz, 1H), 4.79 (s, 2H), 3.96 (t, J = 5.9 Hz, 2H), 3.03 (t, J = 5.8 Hz, 2H). ^{13}C NMR (100 MHz, DMSO-d_6) δ 157.9, 152.8, 145.8, 138.6, 135.3, 135.1, 134.3, 133.4, 128.4, 127.0, 126.5, 126.2, 126.0, 122.9, 120.4, 118.4, 110.1, 108.0, 46.5, 41.8, 28.1. HR-ESI-MS: $[M+H]^+$ *m/z* = 361.1215, calcd for $C_{21}H_{17}ClN_4$, found 361.1197.

4.1.6.9

*2-(6-(6-(trifluoromethyl)-1H-benzo[d]imidazol-2-yl)pyridin-2-yl)-1,2,3,4-tetrahydroisoquinoline (**BD9**).*

Following the general procedure above, **BD9** was obtained as a white solid (36%). ^{1}H NMR (400 MHz, $CDCl_3$) δ 7.75 (d, J = 7.3 Hz, 1H), 7.67 - 7.62 (m, 2H), 7.52 (d, J = 8.2 Hz, 2H), 7.24 - 7.16 (m, 4H), 6.79 (d, J = 8.4 Hz, 1H), 4.78 (s, 2H), 3.93 (t, J = 5.8 Hz, 2H), 3.01 (t, J = 5.7 Hz, 2H). ^{13}C NMR (100 MHz, DMSO-d_6) δ 157.9, 153.7, 145.5, 138.6, 137.0, 135.1, 134.3, 134.0, 128.4, 126.5, 126.2, 126.0, 119.9, 119.4, 116.4, 112.9, 110.2, 109.3, 108.3, 46.5, 41.8, 28.1. HR-ESI-MS: $[M+H]^+$ *m/z* = 395.1478, calcd for $C_{22}H_{17}F_3N_4$, found 395.1455.

4.1.6.10

*6-methoxy-2-(6-(6-methoxy-1H-benzo[d]imidazol-2-yl)pyridin-2-yl)-1,2,3,4-tetrahydroisoquinoline (**BD10**).*

Following the general procedure above, **BD10** was obtained as a light yellow solid (22%). ^{1}H NMR (400 MHz, $CDCl_3$) δ 7.74 - 7.61 (m, 3H), 7.15 (d, J = 8.3 Hz, 1H), 7.03 (brs, 1H), 6.94 (d, J = 8.8 Hz, 1H), 6.80 (d, J = 8.3 Hz, 1H), 6.73 (d, J = 8.4 Hz, 2H), 4.71 (s, 2H), 3.93 (t, J = 5.8 Hz, 2H), 3.88 (s, 3H), 3.81 (s, 3H), 2.99 (t, J = 5.7 Hz, 2H). ^{13}C NMR (100 MHz, DMSO-d_6) δ 157.9, 157.7, 156.2, 150.6, 146.4, 138.5, 136.3, 135.3, 127.5, 126.4, 119.7, 113.0, 112.3, 111.5, 109.2, 107.2, 101.3, 94.6, 55.4, 55.0, 46.1, 41.8, 28.4. HR-ESI-MS: $[M+H]^+$ *m/z* = 387.1816, calcd for $C_{23}H_{22}N_4O_2$, found 387.1793.

4.1.6.11

*6-fluoro-2-(6-(6-fluoro-1H-benzo[d]imidazol-2-yl)pyridin-2-yl)-1,2,3,4-tetrahydroisoquinoline (**BD11**).*

Following the general procedure above, **BD11** was obtained as a light yellow solid (20%). ^{1}H NMR (400 MHz, $CDCl_3$) δ 7.78 - 7.64 (m, 3H), 7.52 - 7.45 (m, 1H), 7.25 - 7.19 (m, 2H), 7.08 - 7.01 (m, 1H), 6.97 - 6.89 (m, 2H), 6.78 (dd, J = 7.9, 4.1 Hz, 1H), 4.76 (s, 2H), 3.94 (t, J = 5.9 Hz, 2H), 3.02 (t, J = 5.8 Hz, 2H). ^{13}C NMR (100 MHz, DMSO-d_6) δ 157.9, 153.1, 147.1 (d, $J_{C\text{-}F}$ = 237.4 Hz), 146.9 (d, $J_{C\text{-}F}$ = 237.4 Hz), 145.4, 138.6, 137.5, 135.0, 134.3, 130.4, 128.4, 126.4, 126.2, 125.9, 110.3, 109.9, 108.4, 108.1, 47.0, 46.4, 28.61. HR-ESI-MS: $[M+H]^+$ *m/z* = 363.1416, calcd for $C_{21}H_{16}F_2N_4$, found 363.1377.

*4.1.6.12 2-(3-(1H-benzo[d]imidazol-2-yl)phenyl)-1,2,3,4-tetrahydroisoquinoline (**B1**).* Following the general procedure above, **B1** was obtained as a white solid (50%). ^{1}H NMR (400 MHz, DMSO-d_6) δ 12.84 (s, 1H), 7.82 (s, 1H), 7.68 (d, J = 7.6 Hz, 1H), 7.60-7.52 (m, 2H), 7.41 (t, J = 7.9 Hz, 1H), 7.30 (d, J = 7.0 Hz, 1H), 7.27 - 7.17 (m, 5H), 7.14 (dd, J = 8.2, 1.6 Hz, 1H), 4.52 (s, 2H), 3.66 (t, J = 5.8 Hz, 2H), 3.00 (t, J = 5.7 Hz, 2H). ^{13}C NMR (100 MHz, DMSO-d_6) δ 151.8, 150.3, 143.7, 134.8, 134.6, 134.2, 130.8, 129.5, 128.3, 126.5, 126.2, 125.8, 122.3, 121.5, 118.7, 116.0, 115.9, 112.0, 111.1, 49.5, 45.4, 28.1. HR-ESI-MS: $[M+H]^+$ *m/z* = 326.1652, calcd for $C_{22}H_{19}N_3$, found 326.1629.

4.1.6.13

*2-(3-(6-fluoro-1H-benzo[d]imidazol-2-yl)phenyl)-1,2,3,4-tetrahydroisoquinoline (**B2**).* Following the general procedure above, **B2** was obtained as a white solid (40%). ^{1}H NMR (400 MHz, $CDCl_3$) δ 7.72 (s, 1H), 7.55 (dd, J = 8.3, 4.5 Hz, 1H), 7.31-7.20 (m, 3H), 7.18 - 7.10 (m, 3H), 7.09 - 7.04 (m, 1H), 6.95-6.87 (m, 2H), 4.40 (s, 2H), 3.54 (t, J = 5.8 Hz, 2H), 2.92 (t, J = 5.7 Hz, 2H). ^{13}C NMR (100 MHz, $CDCl_3$) δ 158.6 (d, J = 195.3 Hz), 153.6, 150.3, 140.4, 134.6, 134.2, 131.6, 129.6, 128.3, 126.5, 126.3, 125.9, 119.6 (d, J = 10.3 Hz), 116.1, 116.0, 112.0, 104.2 (d, J = 23.7 Hz), 97.61 (d, J = 26.5 Hz), 49.5, 45.5, 28.1. HR-ESI-MS: $[M+H]^+$ *m/z* = 344.1558, calcd for $C_{22}H_{18}FN_3$, found 344.1533.

*4.1.6.14 2-(3-(6-chloro-1H-benzo[d]imidazol-2-yl)phenyl)-1,2,3,4-tetrahydroisoquinoline (**B3**).*

Following the general procedure above, **B3** was obtained as a white solid (32%). ^{1}H NMR (400 MHz, DMSO-d_6) δ 7.80 (s, 1H), 7.76 - 7.67 (m, 1H), 7.57 (d, J = 7.7 Hz, 2H), 7.42 (t, J = 7.9 Hz, 1H), 7.32 - 7.14 (m, 6H), 4.53 (s, 2H), 3.67 (t, J = 5.8 Hz, 2H), 3.01 (t, J = 5.7 Hz, 2H). ^{13}C NMR (125 MHz, DMSO-d_6) δ 153.9, 150.8, 135.1, 134.7, 131.0, 130.8, 130.1, 128.8, 128.7, 127.0, 126.9, 126.7, 126.4, 122.6, 116.8, 116.7, 116.5, 112.9, 112.5, 50.0, 45.9, 28.6. HR-ESI-MS: $[M+H]^+$ *m/z* = 360.1262, calcd for $C_{22}H_{18}ClN_3$, found 360.1242.

4.1.6.15

*2-(3-(6-methyl-1H-benzo[d]imidazol-2-yl)phenyl)-1,2,3,4-tetrahydroisoquinoline (**B4**).*

Following the general procedure above, **B4** was obtained as a light yellow solid (40%). ^{1}H NMR (400 MHz, DMSO-d_6) δ 12.67 (d, J = 14.5 Hz, 1H), 7.76 (s, 1H), 7.52 (d, J = 7.4 Hz, 1H), 7.45-7.38 (m, 1H), 7.36 (t, J = 8.0 Hz, 1H), 7.31 - 7.24 (m, 2H), 7.21 - 7.16 (m, 3H), 7.09 (dd, J = 8.2, 2.2 Hz, 1H), 7.04-6.95 (m, 1H), 4.48 (s, 2H), 3.62 (t, J = 5.9 Hz, 2H), 2.96 (t, J = 5.8 Hz, 2H), 2.41 (d, J = 8.4 Hz, 3H). ^{13}C NMR (100 MHz, DMSO-d_6) δ 150.3 (2C), 134.6, 134.3, 130.9, 129.5, 128.3, 127.8, 127.5, 126.9, 126.6, 126.3, 125.9, 123.1, 118.3, 115.9, 115.8, 111.9, 110.9, 49.6, 45.5, 28.2, 21.3. HR-ESI-MS: $[M+H]^+$ m/z = 340.1808, calcd for $C_{23}H_{21}N_3$, found 340.1776.

4.1.6.16

*2-(3-(6-methoxy-1H-benzo[d]imidazol-2-yl)phenyl)-1,2,3,4-tetrahydroisoquinoline (**B5**).*

Following the general procedure above, **B5** was obtained as a white solid (30%). ^{1}H NMR (400 MHz, CD_3OD) δ 7.70 (s, 1H), 7.49-7.39 (m, 2H), 7.35 (t, J = 7.9 Hz, 1H), 7.20 - 7.03 (m, 6H), 6.87 (dd, J = 8.8, 2.3 Hz, 1H), 4.44 (s, 2H), 3.83 (s, 3H), 3.60 (t, J = 5.9 Hz, 2H), 2.97 (t, J = 5.8 Hz, 2H). ^{13}C NMR (125 MHz, DMSO-d_6) δ 155.8, 150.4, 150.3, 134.7, 134.6, 134.3, 134.3, 131.1, 131.0, 129.6, 128.3, 126.5, 126.2, 125.9, 115.9, 115.8, 112.0, 111.8, 55.4, 49.6, 45.5, 28.1. HR-ESI-MS: $[M+H]^+$ m/z = 356.1757, calcd for $C_{23}H_{21}N_3O$, found 356.1732.

4.1.6.17

*2-(3-(6-(trifluoromethyl)-1H-benzo[d]imidazol-2-yl)phenyl)-1,2,3,4-tetrahydroisoquinoline (**B6**).*

Following the general procedure above, **B6** was obtained as a light yellow solid (29%). ^{1}H NMR (400 MHz, $CDCl_3$) δ 7.75 (s, 1H), 7.52 (d, J = 7.5 Hz, 1H), 7.42 - 7.34 (m, 2H), 7.21 - 7.10 (m, 4H), 7.09 - 7.05 (m, 1H), 4.46 (s, 2H), 3.61 (t, J = 5.9 Hz, 2H), 2.97 (t, J = 5.8 Hz, 2H). ^{13}C NMR (100 MHz, $CDCl_3$) δ 155.1, 150.9, 134.8, 134.0, 132.2, 132.0, 130.0 (2C), 128.4 (2C), 126.6 (2C), 126.2 (2C), 119.8, 116.9, 116.4, 116.3, 112.8 (2C), 50.5, 45.9, 29.0. HR-ESI-MS: $[M+H]^+$ m/z = 394.1526, calcd for $C_{23}H_{18}F_3N_3$, found 394.1514.

4.1.6.18

*2-(3-(5,6-dichloro-1H-benzo[d]imidazol-2-yl)phenyl)-1,2,3,4-tetrahydroisoquinoline (**B7**).*

Following the general procedure above, **B7** was obtained as a light yellow solid (32%). ^{1}H NMR (400 MHz, DMSO-d_6) δ 13.16 (s, 1H), 7.92 (s, 1H), 7.74 (d, J = 6.0 Hz, 2H), 7.53 (d, J = 7.3 Hz, 1H), 7.39 (t, J = 7.8 Hz, 1H), 7.29 - 7.08 (m, 5H), 4.48 (s, 2H), 3.61 (d, J = 5.0 Hz, 2H), 2.95 (s, 2H). ^{13}C NMR (100 MHz, DMSO- d_6) δ 154.5, 150.4, 143.5, 134.7, 134.5, 134.2, 129.9, 129.7, 128.3, 126.6, 126.3, 125.9, 124.6, 124.1, 119.8, 116.59, 116.2, 112.6, 112.2, 49.5, 45.5, 28.2. HR-ESI-MS: $[M+H]^+$ *m/z* = 394.0872, calcd for $C_{22}H_{17}Cl_2N_3$, found 394.0860.

4.1.6.19

*2-(3-(5-chloro-6-fluoro-1H-benzo[d]imidazol-2-yl)phenyl)-1,2,3,4-tetrahydroisoquinoline (**B8**).*

Following the general procedure above, **B4** was obtained as a light yellow solid (40%). ^{1}H NMR (400 MHz, DMSO-d_6) δ 7.88 (d, J = 6.9 Hz, 1H), 7.79 - 7.76 (m, 1H), 7.74 - 7.68 (m, 1H), 7.58 – 7.52 (m, 1H), 7.44 - 7.38 (m, 1H), 7.29- 7.27(m, 1H), 7.23 - 7.15 (m, 4H), 4.51 (s, 2H), 3.65 (t, J = 5.9 Hz, 2H), 2.98 (t, J = 5.8 Hz, 2H). ^{13}C NMR (100 MHz, DMSO-d_6) δ 154.5, 154.1, 150.4, 140.6, 134.7, 134.2, 131.7, 130.1, 129.7, 128.3, 126.6, 126.3, 125.9, 119.4, 116.4, 116.1, 112.1, 111.9, 105.6, 49.5, 45.5, 28.1. HR-ESI-MS: $[M+H]^+$ *m/z* = 378.1168, calcd for $C_{22}H_{17}ClFN_3$, found 378.1151.

*4.1.6.20 2-(3-(3,4-dihydroisoquinolin-2(1H)-yl)phenyl)-1H-benzo[d]imidazol-6-ol (**B9**).*

Following the general procedure above, **B5** was obtained firstly and then dissolved in HBr (48% in H_2O). The mixture was stirred at 120 °C for 3 h and then concentrated *in vacuo*. Compound **B9** was obtained as a yellow solid (50%). ^{1}H NMR (400 MHz, CD_3OD) δ 7.77 (s, 1H), 7.65 - 7.60 (m, 2H), 7.53 (d, J = 7.6 Hz, 1H), 7.47 (dd, J = 8.2, 2.1 Hz, 1H), 7.27 - 7.20 (m, 3H), 7.14-7.10 (m, 3H), 4.63 (s, 2H), 3.79 (t, J = 6.0 Hz, 2H), 3.11 (t, J = 5.9 Hz, 2H). ^{13}C NMR (100 MHz, DMSO-d_6) δ 156.5, 150.3, 148.1, 134.6, 134.0, 132.6, 130.5, 128.5, 128.4, 126.6, 126.5, 126.1, 124.7, 123.5, 118.5, 116.2, 114.7, 112.5, 98.0, 49.3, 45.1, 27.9. HR-ESI-MS: $[M+H]^+$ *m/z* = 342.1601, calcd for $C_{22}H_{19}N_3O$, found 342.1574.

4.1.6.21

*2-(3-(3,4-dihydroisoquinolin-2(1H)-yl)phenyl)-1H-benzo[d]imidazol-7-amine (**B10**).*

Following the general procedure above, the intermediate **12** (100 mg, 0.39 mmol) and

1,2-diamino-3-nitrobenzene (66 mg, 0.43 mmol) were reacted. The resulting product, a catalytic amount of Ni and hydrazine hydrate in MeOH were sirred at 50°C for 2 h. After filtration, the solvent was removed under reduced pressure and the pure compound **B10** was obtained as a black solid (41%). ^{1}H NMR (400 MHz, CD_3OD) δ 7.77 (s, 1H), 7.49 (d, J = 7.7 Hz, 1H), 7.43 (t, J = 7.9 Hz, 1H), 7.27 - 7.14 (m, 5H), 7.04 (t, J = 7.8 Hz, 1H), 6.93 (d, J = 7.5 Hz, 1H), 6.58 (d, J = 7.6 Hz, 1H), 4.53 (s, 2H), 3.69 (t, J = 5.8 Hz, 2H), 3.05 (t, J = 5.7 Hz, 2H). ^{13}C NMR (100 MHz, DMSO-d_6) δ 150.8, 150.5, 137.0, 135.1, 134.7, 132.0, 131.6, 130.0, 129.0, 128.8, 127.2, 127.0, 126.7, 126.4, 116.8, 116.6, 116.3, 114.6, 112.3, 50.1, 46.0, 28.7. HR-ESI-MS: $[M+H]^+$ m/z = 341.1761, calcd for $C_{22}H_{20}N_4$, found 341.1734.

4.1.6.22

*6-methoxy-2-(3-(6-methoxy-1H-benzo[d]imidazol-2-yl)phenyl)-1,2,3,4-tetrahydroisoquinoline (**B11**).*

Following the general procedure above, **B11** was obtained as a yellow solid (42%). ^{1}H NMR (400 MHz, $CDCl_3$) δ 7.72 (s, 2H), 7.41 - 7.27 (m, 3H), 7.07 (d, J = 8.4 Hz, 1H), 7.03 (d, J = 8.1 Hz, 1H), 6.97 (s, 1H), 6.92 (dd, J = 8.8, 2.4 Hz, 1H), 6.77 (dd, J = 8.3, 2.5 Hz, 1H), 6.71 (d, J = 2.4 Hz, 1H), 4.43 (s, 2H), 3.87 (s, 3H), 3.80 (s, 3H), 3.61 (t, J = 5.8 Hz, 2H), 2.96 (t, J = 5.7 Hz, 2H). ^{13}C NMR (100 MHz, DMSO-d_6) δ 166.9, 162.7, 148.7, 144.3, 143.9, 141.8, 141.0, 135.3, 133.8, 131.5, 130.5, 129.6, 124.8, 124.3, 123.2, 122.3, 113.5, 112.4, 106.4, 57.2, 55.9, 49.3, 48.6, 28.6. HR-ESI-MS: $[M+H]^+$ m/z = 386.1863, calcd for $C_{24}H_{23}N_3O_2$, found 386.1848.

4.2 Cell culture

As previously described [33], the murine BV-2 microglial cells or HT22 cells (Cell Resource Center of Chinese Academy of Medical Science, Beijing, China) were cultured in Dulbecco's modified Eagle's medium (Gibco) supplemented with 10 % (v/v) fetal bovine serum (Hyclone), 100 U/mL of penicillin, and 100 μg/mL of streptomycin (Hyclone). These cells were cultured in a humidified incubator containing 5% CO_2 at 37°C and subcultured every two days.

4.3 NO production in LPS-stimulated BV2 microglial cells

Microglia cell-based NO inhibitory activity assay were performed as previously described [33]. The BV2 cells were plated in 96-well microplates at a density of 4×10^5 cells/mL (100 μL/well). After 48 h, the medium was removed, and 80 μL of DMEM

was added. The cells were pretreated with various concentrations of compounds (10 μL) for 30 minutes, followed by stimulation with LPS (1 μg/mL, 10 μL, Sigma) for 24 h at 37°C. The same volume (50 μL) of Griess assay agent (Beyotime Biotechnology) was added into the 96-well plates and mixed with the culture medium (50 μL). The mixture solution was incubated at room temperature for 10 min, and the absorbance at 540 nm was measured in a multifunctional microplate reader. The percent of inhibition of NO production was calculated with this formula: $(F_L - F_C)/(F_L - F_0) \times 100\%$, where F_C = absorbance of the cells treated with the tested compound and LPS, F_L = absorbance of the cells treated with LPS, and F_0 = absorbance of the normal cells. The IC_{50} was defined as the concentration of the compound that reduced 50% of NO production with LPS and was calculated by nonlinear regression. All the experiments were repeated independently at least three times.

4.4 Measurement of level of TNF-α and IL-1β production

The procedure is almost the same as above. BV2 cells were plated in 96-well microplates at a density of 4×10^5 cells/mL. After 48 h, the medium was removed, and 80 μL of DMEM was added. The compound solutions (10 μL) were added to the cells firstly, and then 10 μL LPS (1 μg/mL) solution was added. The cells were incubated at 37°C for 24 h. The levels of TNF-*α* and IL-1*β* in the culture medium were measured using ELISA kits (Boster Biological Technology Co. Ltd) according to the manufacturer's instructions.

4.5 MTT assay

The measurement of the cell viability was determined by 3-(4,5-dimethylthiazol-2-yl)-2,5-diphenyltetrazolium bromide (MTT) assay. HT22 cells were plated in 96-well microplates at a density of 5000 cells/well for 24 h, followed by treated with compounds and glutamate (5 mM) for 24 h. After incubation, the cell culture media were removed and 20 μL MTT (5 mg/mL) solution was added to each well and incubated for 4 h at 37°C, after that 120 μL DMSO was added to each well. The absorbance of solubilized formazan was measured by microplate reader at 492 nm. Controls were taken as having 100% viability.

4.6 BACE1 enzymatic assay

According to the previously reported method [29, 35], BACE1 enzymatic activity was determined by the enhancement of fluorescence intensity upon enzymatic cleavage of the fluorescence resonance energy transfer substrate. The human recombinant BACE1 and the substrate peptide (Rh-EVNLDAEFK-Quencher) were purchased from

ThermoFisher Scientific. Briefly, the BACE1 assay was conducted in 50 mM sodium acetate buffer (pH = 4.5), in a final enzyme concentration (1U/mL). The substrate was used at 750 nM. Compounds in DMSO were preincubated with the enzyme for 20 min at room temperature. Subsequently, the substrate was added to initiate the reaction. The reaction was incubated for 60 min at room temperature under dark conditions and then stopped with 2.5 M sodium acetate. Fluorescence intensity was measured by microplate reader at excitation and emission wavelength of 545 nm and 585 nm, respectively.

4.7 BBB permeation assay

The BBB penetration of compounds was evaluated using the parallel artificial membrane permeation assay (PAMPA) described by Di *et al*[32]. Porcine brain lipid (PBL) was obtained from Avanti Polar Lipids. The donor microplate (PVDF membrane, pore size 0.45 mm) and acceptor microplate were both from Millipore. The 96-well UV plate (COSTAR) was from Corning Incorporated. The acceptor 96-well microplate was filled with 300 μL PBS/EtOH/DMSO (68:30:2), and the filter membrane was impregnated with 4 μL PBL in dodecane (20 mg/mL). Compounds were dissolved in DMSO at 5 mg/mL and diluted 50-fold in PBS/EtOH (7:3) to a final concentration of 100 μg/mL. Then, 200 μL of the solution was added to the donor wells. The acceptor filter plate was carefully placed on the donor plate to form a sandwich, which was left undisturbed for 10 h at 25 °C. After incubation, the donor plate was carefully removed, and the concentration of compounds in the acceptor wells was determined using the UV plate reader (Flexstation 3). Every sample was analyzed at five wavelengths in four wells and in at least three independent runs. P_e was calculated by the following expression: $P_e = -V_d \times V_a/[(V_d + V_a)A \times t] \times \ln(1 - \text{drug}_{\text{acceptor}}/\text{drug}_{\text{equilibrium}})$, where V_d is the volume of donor well; V_a, volume in acceptor well; A, filter area; t, permeation time; $\text{drug}_{\text{acceptor}}$, the absorbance obtained in the acceptor well; and $\text{drug}_{\text{equilibrium}}$, the theoretical equilibrium absorbance. The results are given as the mean ± standard deviation. In the experiment, 13 quality control standards of known BBB permeability were included to validate the analysis set. A plot of the experimental data versus literature values gave a strong linear correlation, P_e (exp.) = 1.4574P_e (lit.) − 1.0773 (R^2 = 0.9427). From this equation and the limit established by Di *et al*. (P_e (lit.) = 4.0× 10^{-6} cm/s) for BBB permeation, we concluded that compounds with a permeability > 4.7 × 10^{-6} cm/s could cross the BBB[36].

4.8 Western blot assay

BV-2 cells were seeded on 6-well plates at a density of 30 × 10^4 cells/well for 24 h, incubated with or without **BD3** for 30 minutes, then treated with or without LPS (1 μg/ml) for 16 h. The cell lysates were prepared with RIPA lysis buffer fixed with protease inhibitor cocktail and phosphatase inhibitor. The concentrations of protein were determined by Pierce™ Rapid Gold BCA Protein Assay Kit (ThermoFisher Scientific). A total of 20 μg protein of each sample was electrophoresed in 10% SDS-PAGE, then transferred to polyvinylidene difluoride (PVDF) western membrane (Milipore). The membranes were blocked using 5% (W/V) skim milk in TBST (Tris-buffered saline with 0.1% Tween 20) for 2 h, then the membranes were incubated with primary antibodies at 4°C overnight. Washed by TBST for three times, the membranes were incubated with corresponding secondary antibody at room temperature for 2h. Finally, immunoreactive signals were detected using Chemiluminescence imager (Tanon 5200, Shanghai, China). The anti-iNOS antibody was purchased from Abcam. The anti-α Tubulin antibody was purchased from Cell Signaling Technology.

4.9 RNA isolation and quantitative PCR

Total RNA was isolated using RNAiso plus (TaKaRa) according to the manufacturer's protocol. Total RNA (1μg) was converted to cDNA using ReverTra Ace qPCR RT Master Mix (TOYOBO, code: FSQ-301) according to the manufacturer's protocol. cDNA was used to amplify specific target genes by SYBR Green Real-time PCR Master Mix (TOYOBO, code: QPK-201). The following was the sequences of used PCR primers: iNOS, sense 5′-CCTGGTACGGGCATTGCT-3′ and antisense 5′-GCTCATGCGGCCTCCTTT-3′; IL-1*β*, sense 5′-AAGGGCTGATTCCAAACCTT-TGAC-3′ and antisense 5′-ATACTGCCTGCCTGAAGCTCTTGT-3′; TNF-*α*, sense 5′-TCTCATGCACCACCATCAAGGACT-3′ and antisense 5′-ACCACTCTCCCTTT-GCAGAACTCA-3′; GAPDH, sense 5′-AACTTTGGCATTGTGGAAGG-3′ and antisense 5′-ACACATTGGGGGTAGGAACA-3′. The final results were all normalized as fold change of the target gene/GAPDH.

4.10 Determination of the level of intracellular ROS

HT22 cells were subcultured in 6-well plates at a density of 20 × 10^4 cells/well for 24 h, then treated with 5 mM glutamate in the absence or presence of **BD3** for 12 h.

After that, cells were incubated with 10 μM DCFH-DA for 30 min, washing three times with PBS. Cell fluorescence was immediately recorded using high content screening system (ThermoFisher Scientific) or analyzed by fluorescence microscope (EVOS FL Auto, Life Technologies).

4.11 Measurement of intracellular GSH

GSH level was determined as described the commercial assay kit (Jiancheng Bio.). HT22 cells were subcultured in 6-well plates at a density of 20×10^4 cells/well for 24 h, then treated with 5 mM glutamate in the absence or presence of **BD3** for 12 h. After that, whole-cell lysate was prepared according to the manufacturer's instructions. The amount of proteins was determined using the BCA assay. GSH level was normalized with protein content.

4.12 Docking protocol

The protein target was the *Homo sapiens* BACE1 (*h*BACE1) crystal structure, which was derived from RCSB Protein Data Bank (PDB) (ID: 2B8L). The resolution was 1.7Å. The structure of compound **BD3** was drawn in the ChemDraw with standard bond lengths and angles, and minimized using the MOE. The target was preprocessed with the Protein Preparation Wizard in the Maestro program suite (Schrodinger). The waters beyond 5Å from het groups were deleted. The native ligand in the crystal structure was used to define the binding site. Docking was performed with Glide extra precision (XP) mode (Schrodinger), applying post dock strain penalties. As output options the number of poses per ligand to save was increased to 10. The binding mode in BACE1 was strictly dependent on the protonation state. The figure was prepared using PyMol software.

Conflicts of interest

The authors declare no competing interest.

Acknowledgement

This work was supported in part by the Science and Technology Planning Project of Guangdong Province (2016A020217005), the National Natural Science Foundation of China (81473138, 81001372, 81603030), the Medical Scientific Research Foundation of Guangdong Province (No. A2014212).

References

[1] R.H. Wilkins, I.A. Brody, Alzheimer's disease, Arch Neurol, 21 (1969) 109-110.

[2] D.M. Walsh, D.J. Selkoe, Deciphering the Molecular Basis of Memory Failure in Alzheimer's Disease, Neuron, 44 (2004) 181-193.

[3] Y. Huang, L. Mucke, Alzheimer mechanisms and therapeutic strategies, Cell, 148 (2012) 1204-1222.

[4] X. Du, X. Wang, M. Geng, Alzheimer's disease hypothesis and related therapies, Transl Neurodegener, 7 (2018) 2.

[5] F. Zemek, L. Drtinova, E. Nepovimova, V. Sepsova, J. Korabecny, J. Klimes, K. Kuca, Outcomes of Alzheimer's disease therapy with acetylcholinesterase inhibitors and memantine, Expert Opin Drug Saf, 13 (2014) 759-774.

[6] P. Agostinho, R.A. Cunha, C. Oliveira, Neuroinflammation, oxidative stress and the pathogenesis of Alzheimer's disease, Current Pharmaceutical Design, 16 (2010) 2766.

[7] A. Kumar, A. Singh, Ekavali, A review on Alzheimer's disease pathophysiology and its management: an update, Pharmacol Rep, 67 (2015) 195-203.

[8] H.W. Querfurth, F.M. LaFerla, Alzheimer's disease, N Engl J Med, 362 (2010) 329-344.

[9] M.T. Heneka, M.J. Carson, J. El Khoury, G.E. Landreth, F. Brosseron, D.L. Feinstein, A.H. Jacobs, T. Wyss-Coray, J. Vitorica, R.M. Ransohoff, K. Herrup, S.A. Frautschy, B. Finsen, G.C. Brown, A. Verkhratsky, K. Yamanaka, J. Koistinaho, E. Latz, A. Halle, G.C. Petzold, T. Town, D. Morgan, M.L. Shinohara, V.H. Perry, C. Holmes, N.G. Bazan, D.J. Brooks, S. Hunot, B. Joseph, N. Deigendesch, O. Garaschuk, E. Boddeke, C.A. Dinarello, J.C. Breitner, G.M. Cole, D.T. Golenbock, M.P. Kummer, Neuroinflammation in Alzheimer's disease, The Lancet. Neurology, 14 (2015) 388-405.

[10] J.A. Hardy, G.A. Higgins, Alzheimer's disease: the amyloid cascade hypothesis, Science, 256 (1992) 184-185.

[11] M. Citron, Beta-secretase inhibition for the treatment of Alzheimer's disease--promise and challenge, Trends Pharmacol Sci, 25 (2004) 92-97.

[12] M. Citron, Human beta-secretase and Alzheimer's disease, Expert Opin Ther Targets, 5 (2001) 341-348.

[13] J.D. Scott, S.W. Li, A.P. Brunskill, X. Chen, K. Cox, J.N. Cumming, M. Forman, E.J. Gilbert, R.A. Hodgson, L.A. Hyde, Q. Jiang, U. Iserloh, I. Kazakevich, R. Kuvelkar, H. Mei, J. Meredith, J. Misiaszek, P. Orth, L.M. Rossiter, M. Slater, J. Stone,

C.O. Strickland, J.H. Voigt, G. Wang, H. Wang, Y. Wu, W.J. Greenlee, E.M. Parker, M.E. Kennedy, A.W. Stamford, Discovery of the 3-imino-1,2,4-thiadiazinane 1,1-dioxide derivative verubecestat (MK-8931)-a beta-site amyloid precursor protein cleaving enzyme 1 inhibitor for the treatment of Alzheimer's disease, J Med Chem, 59 (2016) 10435-10450.

[14] F. Prati, A. De Simone, P. Bisignano, A. Armirotti, M. Summa, D. Pizzirani, R. Scarpelli, D.I. Perez, V. Andrisano, A. Perez-Castillo, B. Monti, F. Massenzio, L. Polito, M. Racchi, A.D. Favia, G. Bottegoni, A. Martinez, M.L. Bolognesi, A. Cavalli, Multitarget drug discovery for Alzheimer's disease: triazinones as BACE-1 and GSK-3beta inhibitors, Angew Chem Int Ed, 54 (2015) 1578-1582.

[15] T.A. Dineen, K. Chen, A.C. Cheng, K. Derakhchan, O. Epstein, J. Esmay, D. Hickman, C.E. Kreiman, I.E. Marx, R.C. Wahl, P.H. Wen, M.M. Weiss, D.A. Whittington, S. Wood, R.T. Fremeau, Jr., R.D. White, V.F. Patel, Inhibitors of beta-site amyloid precursor protein cleaving enzyme (BACE1): identification of (S)-7-(2-fluoropyridin-3-yl)-3-((3-methyloxetan-3-yl)ethynyl)-5'H-spiro[chromeno[2, 3-b] pyridine-5,4'-oxazol]-2'-amine (AMG-8718), J Med Chem, 57 (2014) 9811-9831.

[16] W.R. Markesbery, Oxidative stress hypothesis in Alzheimer's disease, Free Radic Biol Med, 23 (1997) 134-147.

[17] J. Godyn, J. Jonczyk, D. Panek, B. Malawska, Therapeutic strategies for Alzheimer's disease in clinical trials, Pharmacol Rep, 68 (2016) 127-138.

[18] A. Cavalli, M.L. Bolognesi, A. Minarini, M. Rosini, V. Tumiatti, M. Recanatini, C. Melchiorre, Multi-target-directed ligands to combat neurodegenerative diseases, J Med Chem, 51 (2008) 347-372.

[19] G. Tsukamoto, K. Yoshino, T. Kohno, H. Ohtaka, H. Kagaya, K. Ito, Synthesis and antiinflammatory activity of some 2-(substituted-pyridinyl)benzimidazoles, J Med Chem, 23 (1980) 734-738.

[20] T.H. Al-Tel, M.H. Semreen, R.A. Al-Qawasmeh, M.F. Schmidt, R. El-Awadi, M. Ardah, R. Zaarour, S.N. Rao, O. El-Agnaf, Design, synthesis, and qualitative structure-activity evaluations of novel beta-secretase inhibitors as potential Alzheimer's drug leads, J Med Chem, 54 (2011) 8373-8385.

[21] Z. Yang, C. Liu, L. Xiang, Y. Zheng, Phenolic alkaloids as a new class of antioxidants in Portulaca oleracea, Phytother Res, 23 (2009) 1032-1035.

[22] H. Sun, X. He, C. Liu, L. Li, R. Zhou, T. Jin, S. Yue, D. Feng, J. Gong, J. Sun, J. Ji, L. Xiang, Effect of oleracein E, a neuroprotective tetrahydroisoquinoline, on

rotenone-induced Parkinson's disease cell and animal models, ACS Chem Neurosci, 8 (2017) 155-164.

[23] M.K. Hu, Y.F. Liao, J.F. Chen, B.J. Wang, Y.T. Tung, H.C. Lin, K.P. Lee, New 1,2,3,4-tetrahydroisoquinoline derivatives as modulators of proteolytic cleavage of amyloid precursor proteins, Bioorg Med Chem, 16 (2008) 1957-1965.

[24] J.W. Seo, E. Srisook, H.J. Son, O. Hwang, Y.N. Cha, D.Y. Chi, Syntheses of tetrahydroisoquinoline derivatives that inhibit NO production in activated BV-2 microglial cells, Eur J Med Chem, 43 (2008) 1160-1170.

[25] D. Zhou, J.L. Gross, A.B. Adedoyin, S.B. Aschmies, J. Brennan, M. Bowlby, L. Di, K. Kubek, B.J. Platt, Z. Wang, G. Zhang, N. Brandon, T.A. Comery, A.J. Robichaud, 2-(Pyrrolidin-1-yl)ethyl-3,4-dihydroisoquinolin-1(2H)-one derivatives as potent and selective histamine-3 receptor antagonists, J Med Chem, 55 (2012) 2452-2468.

[26] Y. Lou, X. Han, A. Kuglstatter, R.K. Kondru, Z.K. Sweeney, M. Soth, J. McIntosh, R. Litman, J. Suh, B. Kocer, D. Davis, J. Park, S. Frauchiger, N. Dewdney, H. Zecic, J.P. Taygerly, K. Sarma, J. Hong, R.J. Hill, T. Gabriel, D.M. Goldstein, T.D. Owens, Structure-based drug design of RN486, a potent and selective Bruton's tyrosine kinase (BTK) inhibitor, for the treatment of rheumatoid arthritis, J Med Chem, 58 (2015) 512-516.

[27] W. Liu, Q. Su, P. Ju, B. Guo, H. Zhou, G. Li, Q. Wu, A hydrazone-based covalent organic framework as an efficient and reusable photocatalyst for the cross-dehydrogenative coupling reaction of N-aryltetrahydroisoquinolines, Chemsuschem, 10 (2017) 664-669.

[28] V.M. Ivanov, The 125th Anniversary of the Griess Reagent, Journal of Analytical Chemistry, 59 (2004) 1002-1005.

[29] Y. Cheng, T.C. Judd, M.D. Bartberger, J. Brown, K. Chen, R.T. Fremeau, Jr., D. Hickman, S.A. Hitchcock, B. Jordan, V. Li, P. Lopez, S.W. Louie, Y. Luo, K. Michelsen, T. Nixey, T.S. Powers, C. Rattan, E.A. Sickmier, D.J. St Jean, Jr., R.C. Wahl, P.H. Wen, S. Wood, From fragment screening to in vivo efficacy: optimization of a series of 2-aminoquinolines as potent inhibitors of beta-site amyloid precursor protein cleaving enzyme 1 (BACE1), J Med Chem, 54 (2011) 5836-5857.

[30] Y. Kang, S. Tiziani, G. Park, M. Kaul, G. Paternostro, Cellular protection using Flt3 and PI3Kalpha inhibitors demonstrates multiple mechanisms of oxidative glutamate toxicity, Nat Commun, 5 (2014) 3672.

[31] J.T. Coyle, P. Puttfarcken, Oxidative stress, glutamate, and neurodegenerative disorders, Science, 262 (1993) 689-695.

[32] L. Di, E.H. Kerns, K. Fan, O.J. McConnell, G.T. Carter, High throughput artificial membrane permeability assay for blood–brain barrier, Eur J Med Chem, 38 (2003) 223-232.

[33] Y.Y. Fang, W.J. Xia, B. Cheng, P. Hua, H.H. Zhou, Q. Gu, J. Xu, Design, synthesis, and biological evaluation of compounds with a new scaffold as anti-neuroinflammatory agents for the treatment of Alzheimer's disease, Eur J Med Chem, 149 (2018) 129-138.

[34] C. Zhao, Y.H. Choi, D.B. Khadka, Y. Jin, K.Y. Lee, W.J. Cho, Design and synthesis of novel androgen receptor antagonists via molecular modeling, Bioorg Med Chem, 24 (2016) 789-801.

[35] T.H. Al-Tel, R.A. Al-Qawasmeh, M.F. Schmidt, A. Al-Aboudi, S.N. Rao, S.S. Sabri, W. Voelter, Rational design and synthesis of potent dibenzazepine motifs as beta-secretase inhibitors, J Med Chem, 52 (2009) 6484-6488.

[36] Z. Wang, Y. Wang, B. Wang, W. Li, L. Huang, X. Li, Design, synthesis, and evaluation of orally available clioquinol-moracin M hybrids as multitarget-directed ligands for cognitive improvement in a rat model of neurodegeneration in Alzheimer's disease, J Med Chem, 58 (2015) 8616-8637.

Highlights

Twenty-two hybrids are designed as multifunctional agents against AD.

Compound **BD3** showed multifunctional activity against neuroinflammation and BACE1.

Compound **BD3** also exhibited significant neuroprotective effect.

The new class of compounds can penetrate BBB and are promising CNS leads.